Surface Structures of Supported Molybdenum Oxide Catalysts: Characterization by Raman and Mo L_3-Edge XANES

Hangchun Hu and Israel E. Wachs*

Zettlemoyer Center for Surface Studies and Departments of Chemistry and Chemical Engineering, Lehigh University, 7 Asa Drive, Bethlehem, Pennsylvania 18015

Simon R. Bare

Catalysis Laboratory, Central Research & Development, The Dow Chemical Company, Midland, Michigan 48674

Received: January 3, 1995; In Final Form: February 24, 1995[⊗]

Supported molybdenum oxide catalysts on TiO_2, Al_2O_3, ZrO_2, SiO_2, and Nb_2O_5 were prepared by the incipient-wetness impregnation method employing aqueous solutions of ammonium heptamolybdate ($(NH_4)_6Mo_7O_{24}{\cdot}4H_2O$). The molecular structures of the surface molybdenum oxide species were investigated by Raman spectroscopy, and their local site symmetries were determined by X-ray absorption near-edge spectroscopy (XANES) at the Mo L_3-edge. Under ambient conditions, the structures of the hydrated surface molybdenum oxide species are controlled by the net surface pH at the point of zero charge (PZC) and are the same as observed in aqueous solutions: MoO_4^{2-}, $Mo_7O_{24}^{6-}$, and $Mo_8O_{26}^{4-}$. Under dehydrated conditions, the structures of the surface molybdenum oxide species depend on both the specific oxide support and surface coverage. At low surface coverages of MoO_3 on Al_2O_3 and TiO_2, the primary species is isolated and tetrahedral coordinated. At high surface coverages of MoO_3, for TiO_2 the primary species is polymerized and octahedral coordinated, but for Al_2O_3 there is a mixture of tetrahedral and octahedral coordinated species. The MoO_3/ZrO_2 system appears to be similar to the MoO_3/Al_2O_3 system, and the MoO_3/Nb_2O_5 system appears to be similar to the MoO_3/TiO_2 system. The surface molybdenum oxide species on SiO_2 is isolated and appears to possess a coordination that is in between tetrahedral and octahedral. Monolayer coverage was achieved at the same surface density of molybdenum oxide on the different oxide supports with the exception of SiO_2. Only low loadings of molybdenum oxide can be dispersed on SiO_2 due to the low concentration and reactivity of the surface OH groups.

Introduction

Supported molybdenum oxide catalysts are widely used in various catalytic processes.[1] The molecular structures of the surface molybdenum oxide species on different oxide supports have been extensively investigated by various techniques over the past decade.[2] Numerous literature studies have concluded from Raman, Fourier transform infrared (FTIR), solid-state ^{95}Mo nuclear magnetic resonance (NMR), extended X-ray absorption fine structure (EXAFS), X-ray absorption near-edge structure (XANES), X-ray photoelectron spectroscopy (XPS), and ultraviolet visible diffuse reflectance spectroscopies (DRS-UV) that the structures of the supported molybdenum oxide species are a function of the specific support, extent of surface hydration and dehydration, surface molybdenum oxide coverage, surface impurities, and calcination temperatures.[2-5] It is now well recognized that the surface structures of the metal oxide overlayers on oxide supports have to be evaluated under two distinctly different environments: ambient and dehydrated conditions. Under ambient conditions, the surface metal oxides are extensively hydrated by water molecules adsorbed on the support surfaces and, therefore, possess structures affected by the surface water. At elevated temperatures, the catalyst surfaces are dehydrated, and the surface metal oxides undergo significant structural changes.[2,4]

The structures of supported molybdenum oxide on Al_2O_3 have been extensively studied under both ambient conditions[6-24] and dehydrated conditions.[25-31] Raman spectroscopy studies[6-11] demonstrated that there are at least three different molybdenum oxide species (tetrahedral and octahedral coordinated surface species as well as a crystalline MoO_3 phase) present on the Al_2O_3 surface under ambient conditions and that their relative concentrations depend on the molybdenum oxide coverage. Subsequent characterization experiments using IR,[12,13] XPS,[13-15] solid-state ^{95}Mo NMR,[16,17] and EXAFS/XANES[18] provided additional information about the three types of Mo species on the Al_2O_3 surfaces under ambient conditions (tetrahedral and octahedral species and MoO_3 crystal phase). Under dehydrated conditions, a highly distorted octahedral molybdenum oxide species at low Mo loadings and a moderately distorted octahedral coordinated molybdenum oxide species (possibly polymeric in nature) at higher Mo loadings were suggested by Raman study to be the surface species present on the Al_2O_3 surface.[28,29]

There recently has been an increasing amount of interest in the MoO_3/SiO_2 catalyst[14,32-55] because of its use as a model catalyst system (especially for selective oxidation reactions). Under ambient conditions, the presence of the polyanionic structures[35-39] and silicomolybdic acid (SMA) Keggin structures[40-43] has been reported. Under dehydrated conditions, the dispersed surface molybdenum oxide species are reported to have either the octahedral structure[32,36-39,44-47] or the tetrahedral structure.[48-50] In comparison to the MoO_3/Al_2O_3 and MoO_3/SiO_2 catalyst systems, relatively few studies have been carried out on the structures of surface molybdenum oxides on TiO_2,[56-65] ZrO_2,[66,67] and Nb_2O_5.[68,69] The molecular structures of these catalyst systems (MoO_3 on TiO_2, ZrO_2, and Nb_2O_5)

* To whom correspondence should be addressed.

[⊗] Abstract published in *Advance ACS Abstracts*, June 15, 1995.

0022-3654/95/2099-10897$09.00/0

TABLE 1: Surface Density of Supported MoO_3 Catalysts at Monolayer Coverage

support	surface area (m^2/g)	monolayer loading (wt % MoO_3)	monolayer surface area (m^2/g)	surface density (Mo atoms/nm^2)
MoO_3				8.0[a]
Al_2O_3	180	20	175	4.6
TiO_2	55	6	53	4.6
ZrO_2	39	4	39	4.3
Nb_2O_5	55	6	47	4.6
SiO_2	380	5	275	0.8[b]

[a] Theoretical monolayer coverage of MoO_3 catalyst from ref 60. [b] Based on monolayer surface area.

are still not well characterized because of the relatively weak Raman signals from the surface Mo oxide species compared to the strong background Raman signals of these oxide supports, especially in the low-frequency region.

Previous attempts at the systematic characterization of molybdenum oxide on different oxide supports[33,34,45,70,71] usually only investigated the structures of molybdenum oxide under ambient conditions,[33] and in some cases even mixed up the hydrated and dehydrated conditions because of laser-induced dehydration.[70,71] There is still a lack of general agreement on the dispersion of the surface molybdenum oxide species on different supports, the structures and coordinations of the surface molybdenum oxide species, and their controlling factors. Therefore, a systematic investigation of the surface molybdenum oxides on different oxide supports is important in order to clarify the confusion surrounding the surface structures of the supported molybdenum oxide catalysts and to reveal their structural dependence on the specific support and hydration/dehydration conditions.

The objectives of this work are (1) to combine Raman and XANES spectroscopies to determine the molecular structures of the surface molybdenum oxide species deposited on different oxide supports (under both ambient and dehydrated conditions), (2) to compare the surface molybdenum oxide monolayer coverage for each support, and (3) for the first time to determine the local site symmetry of the supported molybdenum oxide phases at different Mo loading by using XANES at the Mo L_3-edge. The current findings provide a more complete view of the surface molybdenum oxide species structural dependence on the specific oxide support, their dispersion on different supports, and the effect of hydration/dehydration.

Experimental Section

Catalyst Preparation. The support materials used in this study were TiO_2 (Degussa P-25), ZrO_2 (Degussa), Nb_2O_5 (from $Nb_2O_5 \cdot 4H_2O$, Niobium Products Co., calcined at 773 K for 6 h), Al_2O_3 (Harshaw), and SiO_2 (Cabosil EH-5, water wetted and calcined at 773 K overnight). The BET surface areas of these supports are listed in Table 1. The supported molybdenum oxide catalysts were prepared by the incipient-wetness impregnation method with aqueous solutions of ammonium heptamolybdate ($(NH_4)_6Mo_7O_{24} \cdot 4H_2O$). After impregnation, the samples were dried overnight under ambient conditions and further dried in air at 293 K overnight. The molybdenum oxides supported on TiO_2 and ZrO_2 samples were finally calcined in dry air at 723 K for 2 h, and the molybdenum oxides supported on Nb_2O_5, Al_2O_3, and SiO_2 samples were calcined in dry air at 773 K for 2 h. The molybdenum oxide loading of the catalysts is given as the nominal weight percent of the MoO_3 in the samples. The actual loadings of the catalysts after ICP elemental analysis are listed in Table 2. Only the MoO_3/SiO_2 catalyst possessed slightly less MoO_3 than the deposited MoO_3 loading, and the

TABLE 2: Elemental Analysis of Molybdenum Oxide Contents for Supported Samples

sample	MoO_3 (wt %)	sample	MoO_3 (wt %)
20% MoO_3/Al_2O_3	20.8	5% MoO_3/Nb_2O_5	5.5
5% MoO_3/TiO_2	5.5	4% MoO_3/SiO_2	3.1
5% MoO_3/ZrO_2	5.3		

MoO_3 loading on the other supports are all slightly higher and close to the deposited MoO_3 loading. The BET surface area of the catalysts with monolayer molybdenum oxide coverage are also listed in Table 1. Table 1 shows that the dispersion of molybdenum oxide species is dependent only on the surface area of the oxide supports, except for SiO_2. The deposition of molybdenum oxide on SiO_2 also drastically decreases the surface area of SiO_2.

Raman Spectroscopy. Raman spectra of the supported molybdenum oxide catalysts were obtained with a laser Raman apparatus with the 514.5 nm line of an Ar^+ laser (Spectra Physics, Model 171) as the excitation source. The laser power at each sample was adjusted to ~10 mW for ambient spectral measurements and ~40 mW for the dehydrated sample measurements. The scattered radiation from the sample was directed into a Spex Triplemate spectrometer (Model 1877) coupled to a Princeton Applied Research (Model 1463) OMA III optical multichannel photodiode array detector (1024 pixels). The detector was cooled thermoelectrically to 238 K to decrease the thermal noise. The Raman scattering in the 100−1200 cm^{-1} region was collected, and the spectra were recorded using an OMA III computer and software. The instrument resolution was experimentally determined to be better than 2 cm^{-1}, but the experimental operation and catalyst preparation added additional error and the reproducibility was only better than 4 cm^{-1} found by measuring the same loading samples from various preparations at different times. About 0.2 g of each supported molybdenum oxide catalyst was pressed into a thin wafer of about 1 mm thickness. For the spectral measurements under ambient conditions, a spinning sample holder was used to hold the sample pellet exposed in air and was generally rotated at ~2000 rpm to avoid local heating by the laser beam. For the measurements of the dehydrated samples, a fixed sample holder inside a quartz tube was used which allowed for the continual flowing of dry oxygen gas and heating at ~633 K to dehydrate the samples. The spectra were measured after the samples were fully dehydrated and cooled to room temperature, but the Raman spectrum for supported molybdenum oxide is not dependent on temperature. A scan of the entire vibrational region requires 30 s. Generally, an accumulation of 25 scans was used for stronger Raman signals (Mo on Al_2O_3, TiO_2, ZrO_2, and Nb_2O_5) and 50 scans for weaker Raman signals (Mo on SiO_2). Raman spectra under both hydrated and dehydrated conditions were obtained by subtracting background signals (obtained under no laser beam condition) and correcting for the detector response for different frequency region. To minimize fluorescence from the support, the MoO_3/SiO_2 samples were calcined in dry air at 773 K overnight, and the MoO_3/Al_2O_3 samples were calcined in dry air at 923 K for 2 h before the Raman measurements.

X-ray Absorption Near-Edge Spectroscopy (XANES). Synchrotron radiation-based X-ray absorption near-edge spectroscopy (XANES) at the Mo $l_{2,3}$-edges has previously been demonstrated to provide information on the local site symmetry of dispersed molybdenum oxide surface phases in a series of supported molybdenum oxide on MgO catalysts.[72] This catalyst characterization method was based on some initial data of Mo reference compounds[73] and enzymes.[74] The interpretation of the data is based on an empirical ligand field splitting description

of the final state d-orbital. The initial state of $L_{2,3}$-edge transitions are p-levels, and the dipole-allowed final states are predominantly of d-character. A combination of small natural line widths and high monochromator resolution at 2500 eV results in an estimated 0.5 eV experimental resolution at the Mo $L_{2,3}$-edges. This permits any splitting of the white line at the Mo $L_{2,3}$-edges to be observed. For a tetrahedral coordinated Mo the magnitude of the splitting of the d-orbital is less than that of Mo in an octahedral field (e, t_2 versus t_{2g}, e_g). The number of available orbitals should also be reflected in the relative intensity of each transition. A successful study was performed previously by Bare and co-workers where a direct comparison was made between a series of molybdenum(VI) reference compounds of known structure and the MoO_3/MgO catalysts as a function of weight loading of Mo.[72]

The Mo XANES data were recorded at the National Synchrotron Light Source, Brookhaven National Laboratory, on beam line X19A. The storage ring operated at 2.5 GeV with a current between 110 and 230 mA. The X-ray photons were monochromatized with a NSLS boomerang-type flat crystal monochromator with Si (111) crystals. The slit width of the monochromator was fixed at 3 mm, estimated to give a resolution of 0.5 eV at the Mo L-edges. The harmonic content was reduced by detuning the monochromator crystals by approximately 90%. The X-ray absorption edges were measured as fluorescence yield excitation spectra using a Stern-Heald-Lytle detector with argon as the detector gas. The XANES of the reference compounds were measured as electron yield spectra. To minimize absorption by the air, the path length from the end of the beam pipe to the sample chamber was made as short as possible. Prolene windows (4 μm thick) were used on the Io chamber and entrance window to the *in situ* cell.

The *in situ* EXAFS experiments used a commercially available EXAFS cell[75] which has been described in detail elsewhere.[76] Briefly, the device comprises a water-cooled, helium-flushed aluminum block into which a cylindrical insert for soft X-ray work can be inserted. This cylindrical insert consists of the sample holder and cylindrical housing. The sample holder is made of stainless steel and supports a disk-shaped sample which is heated by a Kanthal resistance heater. The sample holder has a gas inlet and outlet in order to control the gas environment around the sample. The cylindrical housing is water-cooled and has a 5 μm aluminized Mylar window. The gas inlet is connected to a versatile portable feed gas system equipped with electronic mass flow controllers and switching valves.

In the experiments reported here, the catalyst disks (~0.7 g) of each catalyst were pressed and loaded into the sample holder. Mo L-edge XANES spectra were acquired on these air-exposed, hydrated samples. The catalyst disks were then heated to 723 K in a flow of 20% O_2 in He for a given amount of time (usually 30−45 min) in order to dehydrate the samples. Mo L-edge XANES spectra were then acquired at 723 K in the flow of O_2/He. The spectra are normalized to a unit edge jump according to conventional methods. The monochromator was calibrated by setting the first inflection point of the L_3-edge of Mo foil to 2520.0 eV. In this manner the absorption edge of all the catalyst samples falls in the range 4.0−5.0 eV, as expected for Mo(VI) compounds.[72,73] However, chemical shifts have not been used in interpreting the data since the Mo in all of the reference materials and the catalysts is in the +6 oxidation state.

Results

Raman of Supported Molybdenum Oxide Species under Ambient Conditions. The supported molybdenum oxide catalysts possess significant amounts of moisture under ambient conditions, and the surface molybdenum oxide species are in a hydrated environment.[33] The hydrated surface molybdenum oxide species are essentially indistinguishable from those found in aqueous solutions.[2,33] Consequently, the molybdenum oxide aqueous compounds will serve as the reference compounds for the supported molybdenum oxide catalysts under ambient conditions. Table 3 lists the Raman bands of the major aqueous molybdate compounds (MoO_4^{2-}, $Mo_7O_{24}^{6-}$, and $Mo_8O_{26}^{4-}$)[33] as well as their dependence on solution pH; the Raman spectra of these species have previously been reported.[77] The MoO_4^{2-} species is isolated, tetrahedral coordinated and exhibits Raman bands at 897, 837, and 317 cm^{-1}. The $Mo_7O_{24}^{6-}$ and $Mo_8O_{26}^{4-}$ species are polymerized, octahedral coordinated clusters with Raman bands at 943, 903, 570, 362, and 210 cm^{-1} for $Mo_7O_{24}^{6-}$, and $Mo_8O_{26}^{4-}$ possesses Raman bands at 965, 925, 590, 370, and 230 cm^{-1}. The Raman bands in the 890−1000 and 830−970 cm^{-1} region are attributed to the symmetric and asymmetric stretching modes of the terminal Mo=O bond, the bands around 310−370 cm^{-1} are the corresponding bending modes of the terminal Mo=O bond, and the bands at ~560 and 210 cm^{-1} are assigned to the Mo−O−Mo symmetric stretch and Mo−O−Mo deformation modes, respectively. The 570 cm^{-1} band is generally very weak, and the formation of polymerized species is characterized by the presence of the 200−230 cm^{-1} Raman band of the Mo−O−Mo linkage.

TABLE 3: Raman Bands of Molybdate Species in Aqueous Solutions

molybdate species	solution pH	Raman bands (cm^{-1})
MoO_4^{2-}	>8.0	897, 837, 317
$Mo_7O_{24}^{6-}$	6.8−4.8	943, 903, 570, 362, 210
$Mo_8O_{26}^{4-}$	2.2−1.7	965, 925, 590, 370, 230

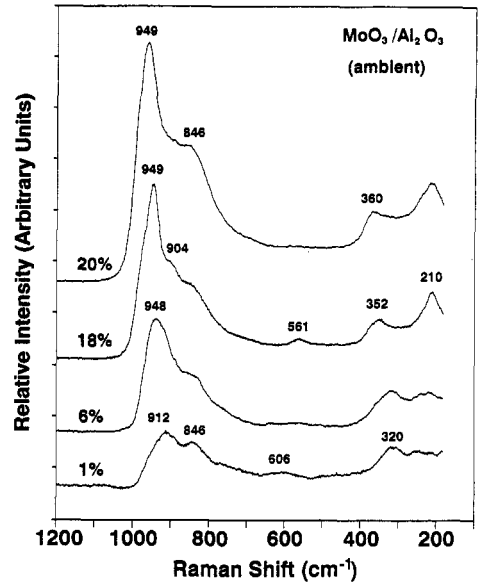

Figure 1. Raman spectra of MoO_3/Al_2O_3 catalysts as a function of MoO_3 loading. Spectra obtained under ambient conditions.

MoO_3/Al_2O_3. The Raman spectra of the 1−20% MoO_3/Al_2O_3 catalysts at ambient conditions are presented in Figure 1. The Raman spectrum of the Al_2O_3 support is essentially featureless in the 100−1200 cm^{-1} region, and the surface molybdenum oxide species on the alumina support possess several Raman bands in the 100−1200 cm^{-1} region. The bands at 912, 846, and 320 cm^{-1} of the 1% MoO_3/Al_2O_3 match fairly well with the Raman bands of tetrahedral coordinated MoO_4^{2-} species in aqueous solutions (see Table 3). The slight upfield shift of the Raman frequencies of the surface molybdenum oxide species

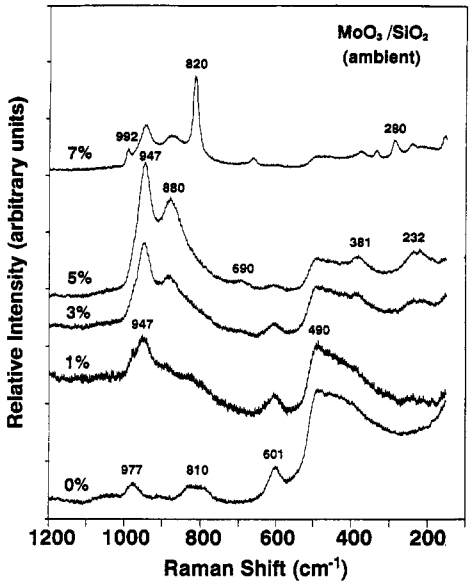

Figure 2. Raman spectra of MoO_3/SiO_2 catalysts as a function of MoO_3 loading. Spectra obtained under ambient conditions.

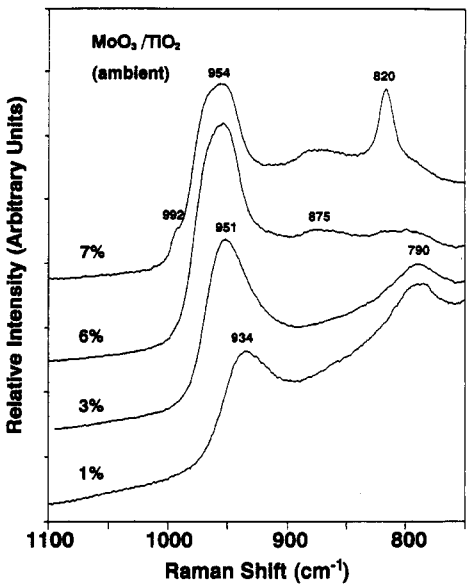

Figure 3. Raman spectra of MoO_3/TiO_2 catalysts as a function of MoO_3 loading. Spectra obtained under ambient conditions.

is probably due to the minor distortion of the hydrated tetrahedral molybdenum oxide structure on the Al_2O_3 surface. Accordingly, the 912, 846, and 320 cm^{-1} can be assigned to the symmetric stretch, asymmetric stretch, and bending modes of hydrated MoO_4 units, respectively.

There are several changes in the Raman features as the molybdenum oxide loading increases from 1% to 20% MoO_3: (a) the major Raman band due to the terminal Mo=O stretch shifts from 912 to 949 cm^{-1}; (b) a new weak band at 561 cm^{-1} appears; (c) the band at 320 cm^{-1} decreases, and a new band at 360 cm^{-1} increases; and (d) the band at 210 cm^{-1} significantly increases. The significant difference in the terminal Mo=O stretching frequency between the 1% and 6% MoO_3/Al_2O_3 samples suggests the presence of different surface molybdenum oxide species. The Raman bands of the higher loading samples are close to that of octahedral coordinated $Mo_7O_{24}^{6-}$ species in aqueous solutions. Thus, the bands observed at 949, 904, and 360 cm^{-1} are attributed to the symmetric stretch, asymmetric stretch, and bending modes of the terminal Mo=O bond of octahedral coordinated MoO_6 species for hydrated $Mo_7O_{24}^{6-}$, respectively.[7] In addition, the Raman bands at 561 and 210 cm^{-1} are assigned to the Mo−O−Mo symmetric stretch and Mo−O−Mo deformation of the MoO_6 unit in hydrated $Mo_7O_{24}^{6-}$, respectively.[28] The higher intensity of the Raman band at 846 cm^{-1} for the high loading ambient MoO_3/Al_2O_3 samples relative to the aqueous $Mo_7O_{24}^{6-}$ species might be due to a slightly different Mo−O−Mo bond angle on the alumina support.[28] The Raman bands due to the hydrated MoO_4^{2-} species disappear, and the bands attributed to the $Mo_7O_{24}^{6-}$ species predominate upon further increasing the Mo loading. These Raman band changes suggest the presence of tetrahedral coordinated species at low Mo loading (hydrated MoO_4^{2-}) and an increase of octahedral coordinated species at higher Mo loading (hydrated $Mo_7O_{24}^{6-}$) under ambient conditions. Strong Raman bands due to crystalline MoO_3 appear for the samples above 20% MoO_3 loading and predominate at higher molybdenum oxide loading samples (not shown in Figure 1) which indicates that monolayer coverage for this Al_2O_3 support (~180 m^2/g) is ~20% MoO_3 loading.

MoO_3/SiO_2. The Raman spectra of the 1−7% MoO_3/SiO_2 catalysts under ambient conditions are presented in Figure 2. The Raman spectrum of SiO_2 possesses broad and weak features at 977, 810, and 601 cm^{-1} and a very broad band from 490 to 380 cm^{-1}. The 977 cm^{-1} band is due to the surface hydroxyl groups (Si−O−H), the 810 and 457 cm^{-1} bands are associated with siloxane linkages, and the 601 and 488 cm^{-1} bands are due to 3- and 4-fold siloxane rings.[38,39] As the molybdenum oxide loading increases, the Raman bands of the surface molybdenum oxide species at 947, 880, 381, and 232 cm^{-1} increase in intensity but do not change positions. The Raman features due to the SiO_2 support decrease in intensity relative to the Raman bands of surface molybdenum oxide species as the molybdenum oxide coverage increases. The Raman features of hydrated surface molybdenum oxide species on SiO_2 match the Raman bands of $Mo_7O_{24}^{6-}$ clusters in aqueous solutions (see Table 3) but are shifted ~20 cm^{-1} to higher frequency with the exception of the 880 cm^{-1} band. This ~20 cm^{-1} shift could be due to a weak interaction between the slightly distorted hydrated $Mo_7O_{24}^{6-}$ clusters and the SiO_2 surface. The relatively high intensity and the somewhat lower band position of the 880 cm^{-1} band suggests that it could arise from more than one vibrational modes. The Mo−O−Mo stretching mode may also contribute to the 880 cm^{-1} band. The maximum dispersion is exceeded when the molybdenum oxide loading is higher than 5% MoO_3, and further addition of molybdenum oxide forms crystalline MoO_3 (major Raman bands at 992, 820, and 280 cm^{-1}). Therefore, molybdenum oxide can be dispersed on this silica support up to 5% MoO_3 loading with the current preparation method. The structure of surface molybdenum oxide species is octahedral coordinated hydrated $Mo_7O_{24}^{6-}$ species at all Mo loadings under ambient conditions.

MoO_3/TiO_2. The Raman spectra of the 1−7% MoO_3/TiO_2 catalysts under ambient conditions are presented in Figure 3. Raman spectra below 700 cm^{-1} were not collected because of the very strong Raman background of the TiO_2 support. The weak band at 790 cm^{-1} is the first overtone of the 395 cm^{-1} band of TiO_2 (anatase),[57] and the relative intensity of this band decreases as the molybdenum oxide coverage increases. The surface molybdenum oxide species possess the terminal Mo=O Raman stretch in the range 934−954 cm^{-1} which shifts to higher frequency as the molybdenum oxide loading increases. The position of the terminal Mo=O stretch at higher Mo loadings suggests the presence of octahedral coordinated surface molybdenum oxide species with a structure similar to that of $Mo_7O_{24}^{6-}$ or $Mo_8O_{26}^{4-}$ clusters in aqueous solutions. At lower Mo loading, the Raman band position of the terminal Mo=O

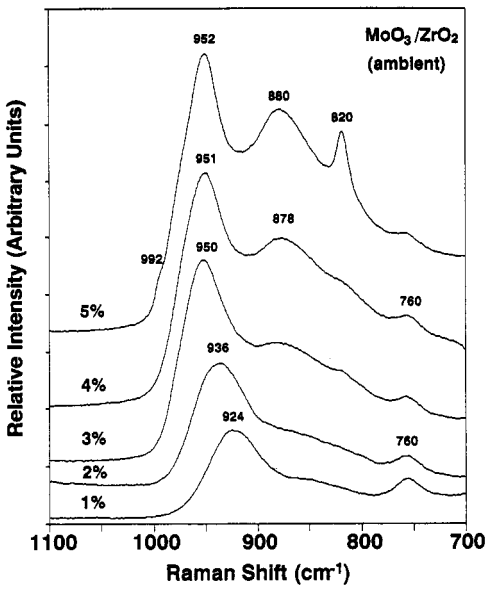

Figure 4. Raman spectra of MoO_3/ZrO_2 catalysts as a function of MoO_3 loading. Spectra obtained under ambient conditions.

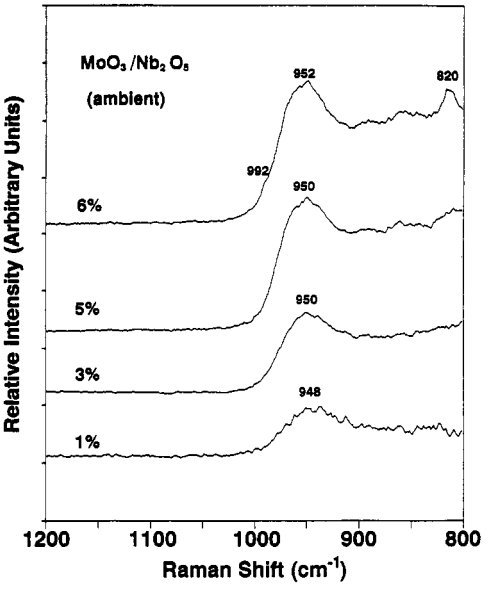

Figure 5. Raman spectra of MoO_3/Nb_2O_5 catalysts as a function of MoO_3 loading. Spectra obtained under ambient conditions.

bond also suggests the presence of a tetrahedral hydrated MoO_4^{2-} component. A weak and broad band at ~875 cm^{-1} also increases in intensity as the molybdenum oxide coverage increases. The 875 cm^{-1} Raman band is probably due to the stretching mode of a Mo−O−Mo bond of the polymerized three-dimensional surface molybdenum oxide species (hydrated $Mo_8O_{26}^{4-}$ or $Mo_7O_{24}^{6-}$).[28] Strong Raman bands of crystalline MoO_3 are present at 820 and 992 cm^{-1} for the 7% MoO_3/TiO_2 (55 m^2/g) sample which indicates that monolayer coverage of the surface molybdenum oxide species has been exceeded.

MoO_3/ZrO_2. The Raman spectra of the 1−5% MoO_3/ZrO_2 catalysts under ambient conditions are presented in Figure 4. Raman spectra below 700 cm^{-1} were not collected due to the strong background of the ZrO_2 support. The weak band at 760 cm^{-1} is due to ZrO_2 support and decreases in relative intensity as the molybdenum oxide coverage increases. The Mo=O terminal Raman stretch for the 1% sample (924 cm^{-1}) suggests the presence of tetrahedral species. The Raman band position increases to 952 cm^{-1} as the molybdenum oxide coverage increases from 1% to 5% MoO_3, which corresponds to the range of the terminal stretching bands of polymolybdate species (hydrated $Mo_7O_{24}^{6-}$ and $Mo_8O_{26}^{4-}$). The broad band around 880 cm^{-1} increases with coverage and increases further after reaching monolayer coverage as shown for the 5% MoO_3/ZrO_2 sample. Thus, the molybdenum oxide monolayer on the ZrO_2 support at higher Mo loading possesses hydrated surface hepta- and octamolybdate species under ambient conditions. Monolayer coverage for the surface molybdenum oxide species on this ZrO_2 (39 m^2/g) support is ~4% MoO_3 loading since crystalline MoO_3 (major Raman bands at 820 cm^{-1}) is present at higher loadings.

MoO_3/Nb_2O_5. The Raman spectrum of bulk niobium oxide possesses strong Raman bands at ~690 cm^{-1}, a shoulder at ~820 cm^{-1}, and bands at ~300 and 220 cm^{-1} which are also quite intense. Thus, Raman spectra of the MoO_3/Nb_2O_5 catalysts below 800 cm^{-1} were not collected because the very strong scattering from the Nb_2O_5 support dominates this region. The surface molybdenum oxide Raman features are quite weak against the strong Nb_2O_5 background, and thus, the peak positions of surface niobium oxide species are difficult to determine precisely. The Raman spectra of the 1−6% MoO_3/Nb_2O_5 catalysts under ambient conditions shown in Figure 5 were obtained by subtracting the spectrum of the Nb_2O_5 support background in order to enhance the surface molybdenum oxide signals. The major Raman bands for the Mo=O stretch increase slightly from 943 to 952 cm^{-1} as the molybdenum oxide coverage increases. The band position for the terminal Mo=O stretching mode suggests that the surface molybdenum oxide species is primarily present as polymolybdate species (hydrated $Mo_7O_{24}^{6-}$ and $Mo_8O_{26}^{4-}$) on the Nb_2O_5 support. The small 820 cm^{-1} band and a weak shoulder at 992 cm^{-1} characteristic of crystalline MoO_3 appear for 6% MoO_3/Nb_2O_5 sample, which indicates that monolayer coverage for surface molybdenum oxide species has been slightly exceeded. Thus, the monolayer coverage of molybdenum oxide on this Nb_2O_5 support (55 m^2/g) is ~6% MoO_3, and the structure of the hydrated surface molybdenum oxide species is similar to hydrated $Mo_7O_{24}^{6-}$ and $Mo_8O_{26}^{4-}$ clusters under ambient conditions.

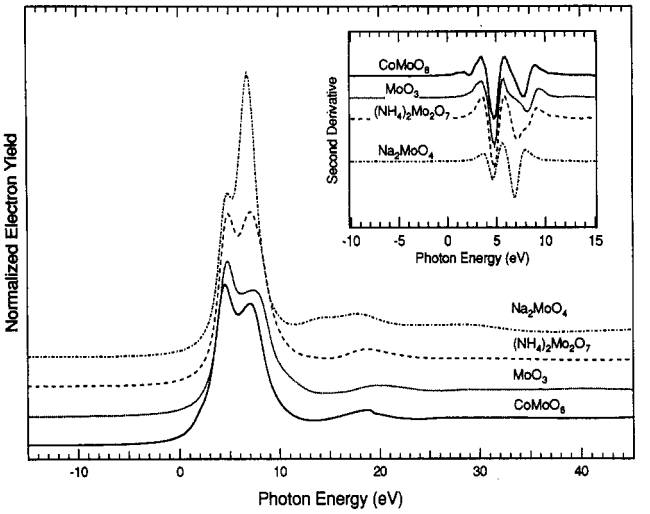

Figure 6. Fluorescence yield Mo L_3-edge XANES of a series of Mo(VI) reference compounds. The spectra have been normalized as described in the text. The inset shows the second derivative of the spectra. In both cases the vertical scale is offset for clarity.

XANES Spectra of Reference Compounds and Hydrated Catalysts. The Mo L_3-edge XANES, shown as electron yield signals, of a series of reference compounds, $CoMoO_6$, MoO_3, $(NH_4)_2Mo_2O_7$, and Na_2MoO_4, are shown in Figure 6. The prominent feature in the spectra is the intense white line. At the Mo L_3-edge this white line is a result of transitions from

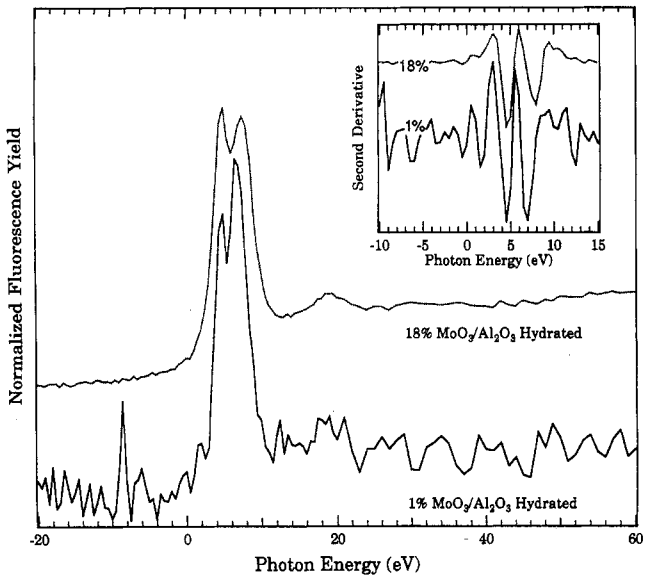

Figure 7. Fluorescence yield Mo L_3-edge XANES of ambient 1% (solid line) and 18% (dotted line) MoO_3/Al_2O_3 catalysts at room temperature. The spectrum of the 1% MoO_3/Al_2O_3 sample has been normalized to the height of the white line of the 18% sample due to problems with background subtraction for the low loading sample. The inset shows the second derivative of the spectra. In both cases the vertical scale is offset for clarity.

the dipole-allowed 2p → 4d transition. In addition, splitting of the line is observed, reflecting the ligand field splitting of the final state d-orbital.[73,74] The magnitude, and relative intensity, of the splitting can be understood using simple ligand field concepts. In a tetrahedral field the magnitude of the splitting of the d-orbital is smaller than in an octahedral field (e, t_2 versus t_{2g}, e_g). The number of available orbitals is also consistent with the relative intensities observed (e, 2 and t_2, 3; t_{2g}, 3 and e_g, 2).[73,74] In $CoMoO_6$ and MoO_3 the Mo is octahedral coordinated to six oxygen atoms, whereas in Na_2MoO_4 the Mo is tetrahedral coordinated. $(NH_4)_2Mo_2O_7$ has Mo atoms both tetrahedral and octahedral coordinated to oxygen. Both the magnitude of the splitting and relative intensity of the peaks of the compounds shown in Figure 6 are consistent with their symmetry. The fluorescence yield data for these compounds have previously been shown, but here the magnitudes are free of thickness effects.[72] The inset of Figure 6 shows the second derivatives of the XANES which serve to highlight the differences between the spectra. The range of values for the splitting of tetrahedral coordinated Mo oxides is 1.8−2.4 eV, whereas for octahedral coordinated Mo oxides it is 3.1−4.5 eV.[72]

The Mo XANES data under hydrated conditions indicate that there are significant differences in the local site symmetry of molybdenum oxide supported on alumina, titania, and silica which depend on both the oxide support and surface coverage. The Mo L_3-edge XANES of 1 and 18 wt % MoO_3/Al_2O_3 catalysts in the ambient state are shown in Figure 7. The inset shows the second derivatives of the XANES. The measured splitting of the peaks in the second derivative of 1% MoO_3/Al_2O_3 is 2.25 eV, and that of the 18% MoO_3/Al_2O_3 is 3.5 eV. The intensity ratio of the first to second peaks is reversed between the two samples. In the 1% MoO_3/Al_2O_3 case the second peak is larger than the first, and for the 18% MoO_3/Al_2O_3 catalyst the first is slightly larger than the second. For the 1% MoO_3/Al_2O_3 catalyst both the splitting of the peaks and their relative intensity indicate that the molybdenum oxide species is tetrahedral coordinated. The XANES spectrum of the 18% MoO_3/Al_2O_3 under ambient conditions suggests that the coordination of the surface molybdenum oxide species in this sample appears to be octahedral coordinated, as evidenced both by the large splitting of the peaks and their relative intensity ratio. Thus, the coordination of the surface molybdenum oxide species on Al_2O_3 changes from tetrahedral to octahedral with increasing Mo coverage under ambient conditions.

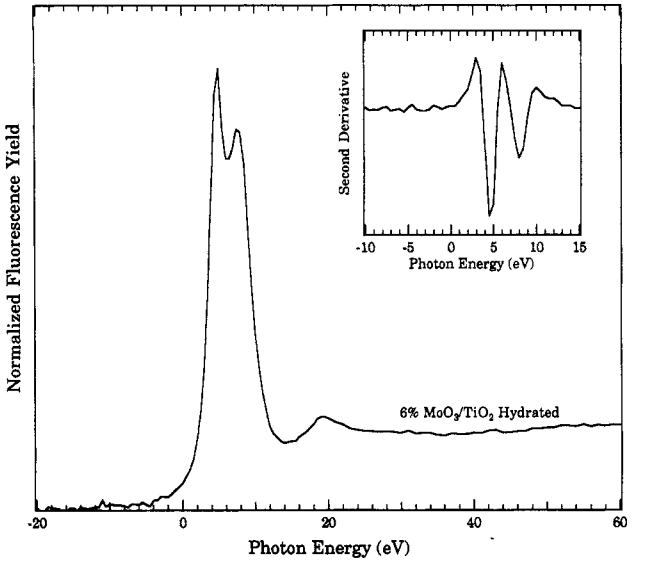

Figure 8. Fluorescence yield Mo L_3-edge XANES of an ambient 6% MoO_3/TiO_2 catalyst at room temperature. The inset shows the second derivative of the spectrum.

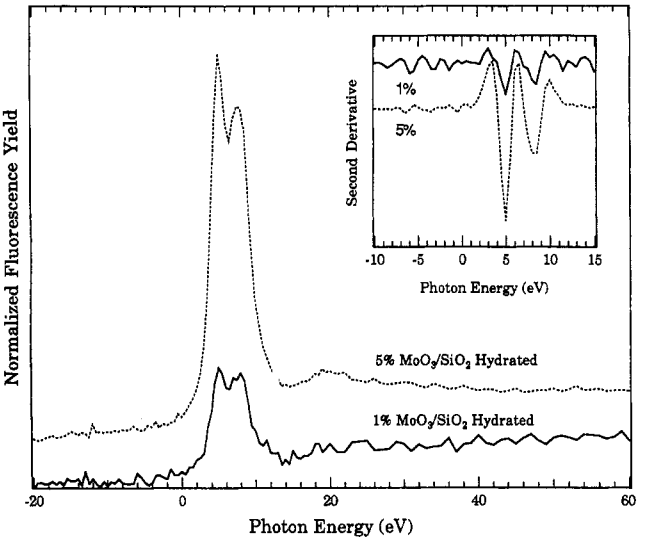

Figure 9. Fluorescence yield Mo L_3-edge XANES of ambient 1% (solid line) and 5% (dotted line) MoO_3/SiO_2 catalysts at room temperature. The white line intensity of the 1% sample is reduced due to problems with background subtraction for the low loading sample. The inset shows the second derivative of the spectra. In both cases the vertical scale is offset for clarity.

The Mo L_3-edge XANES data for the 6% MoO_3/TiO_2 sample under ambient conditions are shown in Figure 8. No data were collected for the low-coverage MoO_3/TiO_2 catalyst in its hydrated state. The spectrum shows a splitting of ~3.2 eV with the first peak larger than the second and is consistent with an octahedral coordination of the hydrated surface molybdenum oxide species on TiO_2 at monolayer coverage. Therefore, the molybdenum oxide species on TiO_2 is octahedral coordinated at monolayer coverage under ambient conditions.

The 1% and 5% MoO_3/SiO_2 Mo L_3-edge XANES spectra and the corresponding second derivatives, shown as the inset, are presented in Figure 9. The splitting of the white line is 3.5 eV for the 1% MoO_3/SiO_2 catalyst and 3.25 eV for the 5%

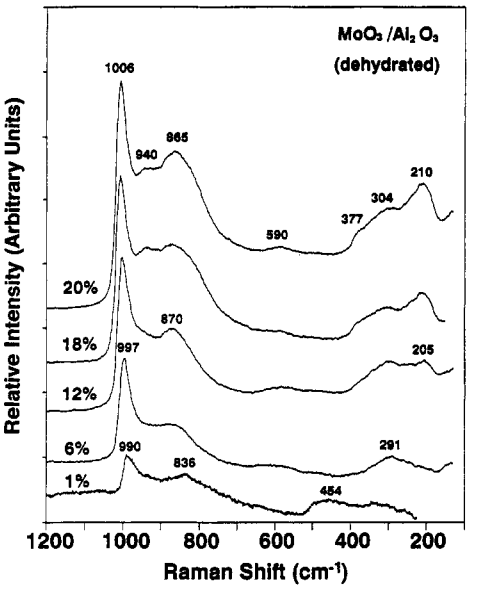

Figure 10. Raman spectra of MoO_3/Al_2O_3 catalysts as a function of MoO_3 loading. Spectra obtained under dehydrated conditions.

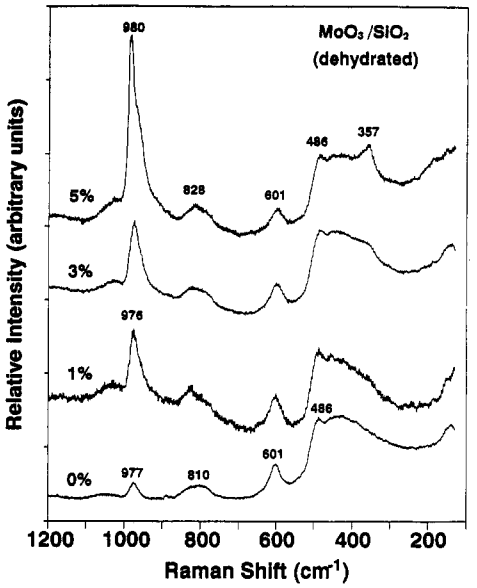

Figure 11. Raman spectra of MoO_3/SiO_2 catalysts as a function of MoO_3 loading. Spectra obtained under dehydrated conditions.

MoO_3/SiO_2 sample. In both cases the intensity of the first peak is larger than the second. From the splitting of the peaks at the white line and their relative intensity ratio the surface molybdenum oxide is octahedral coordinated at both low and high molybdenum oxide loadings. Thus, the coordination of the hydrated surface molybdenum oxide species is octahedral on SiO_2 at all coverages under ambient conditions.

Raman of Supported Molybdenum Oxide Species under Dehydrated Conditions. Solid molybdate compounds possess both tetrahedral and octahedral coordination with the high-frequency Raman bands ranging from 840 to 1060 cm^{-1} for the terminal Mo=O stretching modes. In general, higher frequencies of the Mo=O stretch suggest shorter Mo=O bonds and greater distortions in the structure.[78,79] Raman frequencies in the 200−300 and 500−800 cm^{-1} regions are associated with Mo−O−Mo functionalities. The surface molybdenum oxide species on oxide supports, however, possess structures that are generally different from those found in bulk molybdenum oxide compounds, and consequently, appropriate model reference compounds are not available for the surface molybdate. The Raman spectra of the supported molybdenum oxide species under dehydrated conditions provide information about specific bond functionalities (Mo=O, Mo−O−Mo, etc.) but cannot determine the Mo coordination because of the unavailability of surface molybdate reference compounds.

MoO_3/Al_2O_3. The Raman spectra of the MoO_3/Al_2O_3 catalysts as a function of molybdenum oxide loading under dehydrated conditions are presented in Figure 10. At all MoO_3 loadings, a sharp Raman band in the terminal Mo=O stretching region at ~1000 cm^{-1} and a weak Raman band in the Mo=O bending region at ~300 cm^{-1} are observed. With increasing molybdenum oxide loading, the sharp Raman band increases in intensity and shifts from 990 to 1006 cm^{-1} while a broad band at ~870 cm^{-1} also increases in intensity. The Raman spectrum of the 1% MoO_3/Al_2O_3 sample also possesses a broad band at 836 cm^{-1} and a band at 454 cm^{-1} which is due to the instrumental background.[28] The Raman spectra of the higher Mo loaded samples reveal additional bands at ~940, ~590, ~377, and ~210 cm^{-1}. The presence of the 210 and 590 cm^{-1} bands, characteristic of Mo−O−Mo vibrations, for the 12−20% samples indicates the presence of surface polymolybdate species for these higher molybdenum oxide loading samples. The high wavenumber shift of the terminal stretching band (990−1000 cm^{-1}) and the absence of the ~210−220 cm^{-1} band for the low Mo loading samples (1% and 6% MoO_3/Al_2O_3) suggest the presence of a highly distorted and isolated dehydrated surface species.[80] The Raman bands at ~940, 590, ~377, and 210 cm^{-1} for the high loading samples (12−20% MoO_3/Al_2O_3) are an indication of the presence of highly distorted surface polymolybdate species under dehydrated conditions.

MoO_3/SiO_2. The Raman spectra of the MoO_3/SiO_2 catalysts under dehydrated conditions as a function of MoO_3 loading are presented in Figure 11. The terminal Mo=O stretching band is located in the 976−980 cm^{-1} region. The 977 cm^{-1} Raman band of the Si−O−H stretching mode is gradually replaced by the 980 cm^{-1} Raman band of the surface molybdenum oxide species. The asymmetric nature of this terminal band implies an unresolved shoulder at ~970 cm^{-1}. The 970 cm^{-1} band is more pronounced in samples from nonaqueous preparations[38] that achieved higher dispersions of molybdenum oxide on SiO_2. The 970 cm^{-1} band was also reported in an IR study[46] and was assigned to a second surface molybdenum oxide species. The Raman spectrum of the 5% MoO_3/SiO_2 sample also exhibits a band at 357 cm^{-1} which is due to the bending mode of the terminal Mo=O bond. The absence of the Mo−O−Mo deformation mode at ~220 cm^{-1} for all Mo loaded samples suggests that only isolated surface molybdenum oxide species is present on SiO_2 surfaces. There is a weak band at ~1040 cm^{-1} that increases with molybdenum oxide loading that originated from surface Si−O^- functionalities[38] formed during the anchoring of the surface molybdenum oxide species to the SiO_2 support. Thus, the dehydrated surface molybdenum oxide species on SiO_2 possess an isolated and highly distorted structure.

MoO_3/TiO_2. The Raman spectra of the MoO_3/TiO_2 catalysts under dehydrated conditions as a function of molybdenum oxide loading are presented in Figure 12. The Raman stretching mode of the terminal Mo=O bond is sharp and occurs at 993−998 cm^{-1}, which suggests a highly distorted structure. A very weak and broad band at ~910 cm^{-1} increases as the molybdenum oxide loading increases and is assigned to the formation of polymerized surface molybdenum oxide species. There is no direct information about whether Mo−O−Mo linkages exist in the dehydrated surface molybdenum oxide species on TiO_2 because it is not possible to obtain Mo−O vibrational informa-

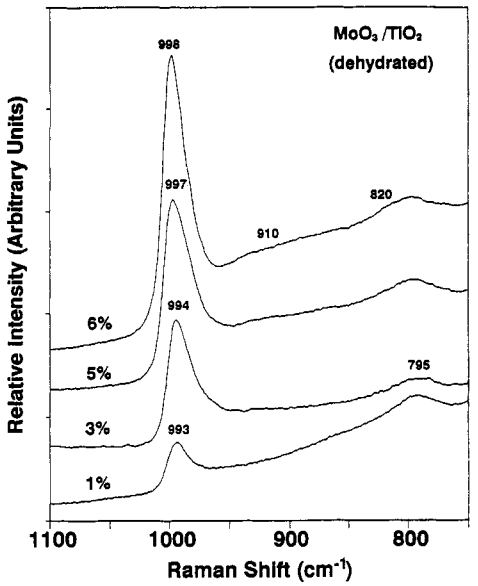

Figure 12. Raman spectra of MoO_3/TiO_2 catalysts as a function of MoO_3 loading. Spectra obtained under dehydrated conditions.

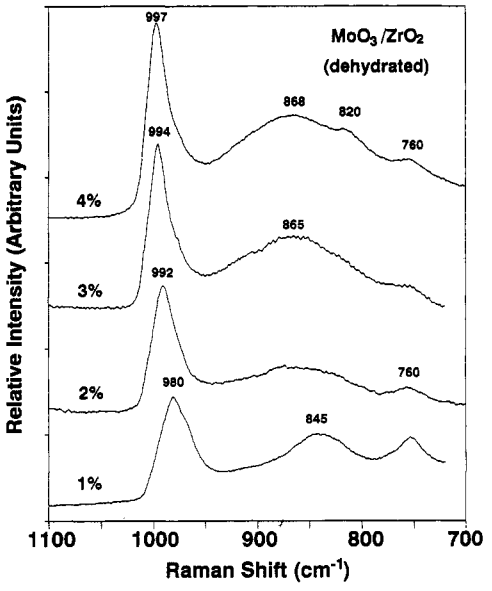

Figure 13. Raman spectra of MoO_3/ZrO_2 catalysts as a function of MoO_3 loading. Spectra obtained under dehydrated conditions.

tion below 700 cm^{-1} due to the strong Raman scattering of the TiO_2 support.

MoO_3/ZrO_2. The Raman spectra of the MoO_3/ZrO_2 catalysts as a function of molybdenum oxide loading under dehydrated conditions are presented in Figure 13. The stretching mode of the terminal Mo=O bond shifts from 980 to 997 cm^{-1} as the molybdenum oxide loading increases. At low molybdenum oxide coverage (1% MoO_3/ZrO_2), there is also a broad Raman band at 845 cm^{-1} along with the major 980 cm^{-1} band. As the molybdenum oxide coverage increases, the 845 cm^{-1} Raman band shifts to ~868 cm^{-1}. There is no Raman information about the low-frequency region for the MoO_3/ZrO_2 catalysts due to the strong Raman scattering from the ZrO_2 support. However, comparison of the Raman spectra of the MoO_3/ZrO_2 catalysts with the corresponding MoO_3/Al_2O_3 catalysts reveals a similarity between them. Therefore, similar surface molybdenum oxide structures appear to be present on the ZrO_2 surface as that on the Al_2O_3 surface, *e.g.*, highly distorted, isolated surface molybdenum oxide species present on the ZrO_2 surfaces

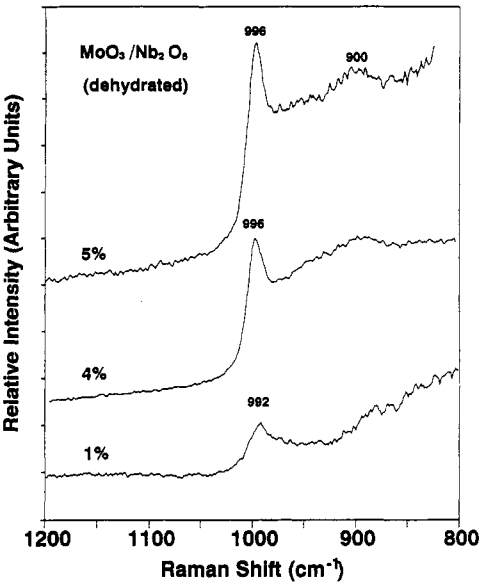

Figure 14. Raman spectra of MoO_3/Nb_2O_5 catalysts as a function of MoO_3 loading. Spectra obtained under dehydrated conditions.

for low loadings and distorted, polymerized surface molybdenum oxide species present on ZrO_2 at high loadings.

MoO_3/Nb_2O_5. The Raman spectra of the MoO_3/Nb_2O_5 catalysts as a function of molybdenum oxide loading under dehydrated conditions, after subtraction of the Nb_2O_5 support background, are presented in Figure 14. The terminal Mo=O stretching Raman band shifts from 992 to 996 cm^{-1} with increasing Mo oxide coverage. A broad and weak band at ~900 cm^{-1} is also present and its intensity also increases as the molybdenum oxide loading increases. As above, the ~996 cm^{-1} Raman band can be assigned to the terminal Mo=O stretch mode of a dehydrated highly distorted surface molybdenum oxide species, and the weak ~900 cm^{-1} Raman band is possibly due to the presence of polymolybdate species. The strong Raman scattering of the Nb_2O_5 support in the low-frequency region prevents the collection of additional information about the surface molybdenum oxide species on Nb_2O_5.

XANES Studies of the Dehydrated Catalysts. The previously calcined catalyst wafers were dehydrated *in situ* by flowing dry 20% O_2 in He over the samples as they were heated to 723 K. After approximately 30−45 min, the Mo L_3-edge XANES was recorded on each catalyst at 723 K in the flow of O_2/He. The spectra for the 1% and 18% MoO_3/Al_2O_3 samples are shown in Figure 15. The inset shows the second derivatives of the XANES spectra shown in the main figure. The splitting of the two peaks for the 1% MoO_3/Al_2O_3 catalyst is 2.5 eV, and that for the 18% catalyst is 2.9 eV. The intensities of the split peaks in the white line for the high-loading alumina-supported sample are of comparable magnitude. In fact, the overall spectrum is quite similar to that of diammonium dimolybdate ($(NH_4)_2Mo_2O_7$), shown in Figure 6. For the dehydrated 1% MoO_3/Al_2O_3 catalyst the second peak is still larger than the first, as in the hydrated case. Thus, the dehydrated 1% MoO_3/Al_2O_3 appears to possess tetrahedral coordinated surface molybdenum oxide species, and the dehydrated 18% MoO_3/Al_2O_3 appears to possess a mixture of tetrahedral and octahedral coordinated surface molybdenum oxide species.

The Mo L_3-edge XANES data for the dehydrated titania-supported catalysts are shown in Figure 16. The XANES spectra of the 1% MoO_3/TiO_2 and the 6% MoO_3/TiO_2 catalysts are quite different. For the 1% MoO_3/TiO_2 catalyst the measured splitting in the second derivative is 2.3 eV, with the second peak larger than the first in the normalized data. For

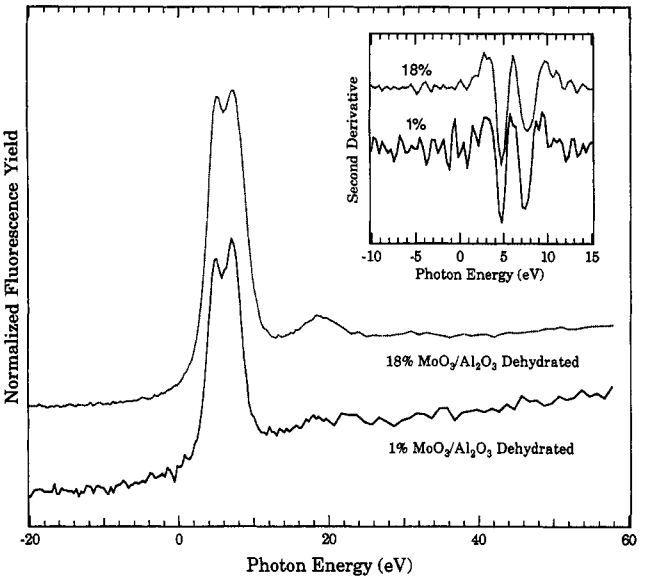

Figure 15. Fluorescence yield Mo L_3-edge XANES of dehydrated 1% (solid line) and 18% (dotted line) MoO_3/Al_2O_3 catalysts at 723 K. The inset shows the second derivative of the spectra. In both cases the vertical scale is offset for clarity.

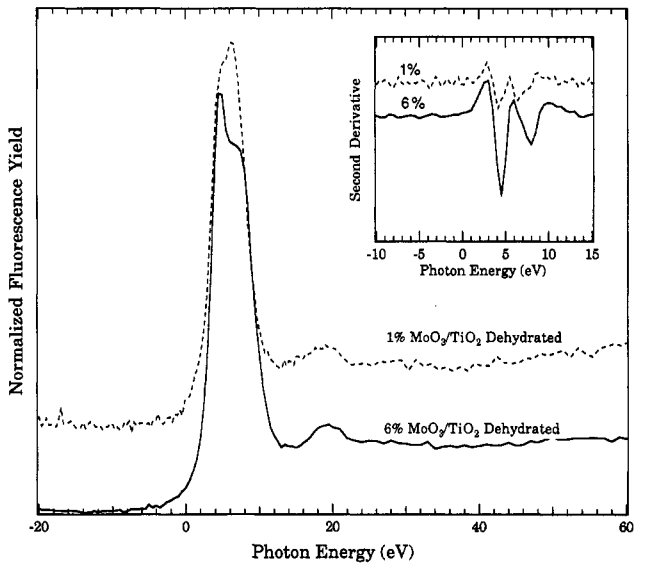

Figure 16. Fluorescence yield Mo L_3-edge XANES of dehydrated 1% (solid line) and 6% (dotted line) MoO_3/TiO_2 catalysts at 723 K. The inset shows the second derivative of the spectra.

the 6% MoO_3/TiO_2 sample, the spectrum looks quite similar to that of bulk MoO_3, shown in Figure 6, and the splitting between the two peaks is 3.5 eV. The first peak is also larger than the second. Thus, the dehydrated 1% MoO_3/TiO_2 possesses a structure with tetrahedral coordination, and the dehydrated 6% MoO_3/TiO_2 possesses an octahedral coordinated surface molybdenum oxide species.

In situ Mo L_3-edge XANES data were collected on three different weight loading of the MoO_3/SiO_2 catalysts. The 1% and 5% MoO_3/SiO_2 catalysts were prepared by the aqueous impregnation method in our laboratory, while the 3.5% sample was supplied from a different group and was prepared from a molybdenum allyl compound.[37] As shown in Figure 17, the spectra of all three catalysts are identical. There is no clear splitting of the white line at the Mo L_3-edge, although the asymmetry of the white line clearly indicates the presence of two peaks. The second derivatives are shown in the inset of Figure 17. The peaks in the second derivative indicate a "splitting" of ~2.8 eV. Thus, the dehydrated surface structure

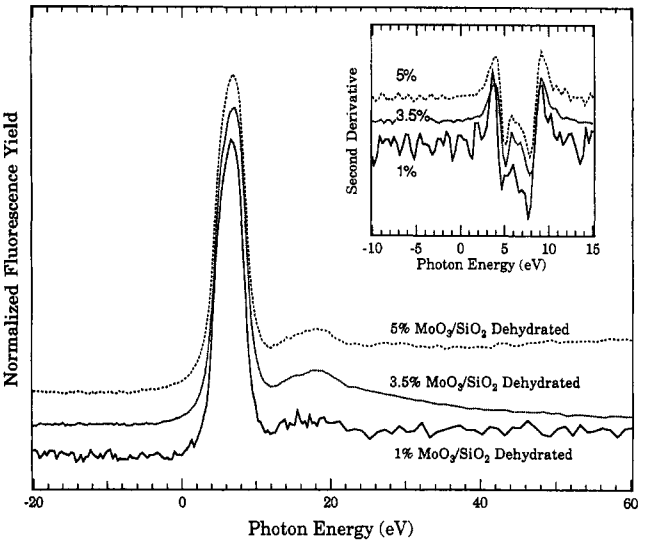

Figure 17. Fluorescence yield Mo L_3-edge XANES of dehydrated 1% (solid line), 3.5% (dotted line), and 5% (dashed line) MoO_3/SiO_2 catalysts at 723 K. The spectra have all been normalized to the same intensity white line. The inset shows the second derivative of the spectra. In both cases the vertical scale is offset for clarity.

of the MoO_3/SiO_2 catalysts is not simply tetrahedral or octahedral coordinated and may possess a coordination in between MoO_4 and MoO_6 units.

Discussion

Surface Structures of Supported Molybdenum Oxides under Ambient Conditions. Molybdenum oxide ions are known to form isopolyanions in aqueous solutions, and the state of aggregation in these solutions is highly dependent on pH and Mo concentration.[2,33] Above a pH of 8.0, isolated and tetrahedrally coordinated MoO_4^{2-} is the major species present in aqueous solution. For pH values between 4.8 and 6.8, the predominate species is a polymerized and octahedrally coordinated $Mo_7O_{24}^{6-}$ cluster. For pH values of 1.7−2.2, octahedral $Mo_8O_{26}^{4-}$ species is the main species in aqueous solution (see Table 3).

The point of zero charge (PZC) of a supported metal oxide catalyst system depends on both the oxide support and the molybdenum oxide loading since the addition of molybdenum oxide decreases the surface pH of the oxide support (PZC of MoO_3 ~2.3).[81] It has been proposed that the final pH of the solutions in the filled pores of support is close to the PZC of the support because of the fairly large buffer capacity of the support.[9] However, directly following the dependence of the PZC of the catalysts on the molybdenum oxide loading for MoO_3/Al_2O_3 catalysts by Kohler *et al.*[23] found that the PZC of the catalysts continuously decreases from ~9 to 3.8 as the molybdenum oxide loading increases from 0 to ~10% Mo loading. This decrease in the PZC is responsible for the structural changes from tetrahedral to octahedral coordinated hydrated molybdenum oxide species which is analogous to the structures formed by molybdenum oxide in an aqueous solution possessing solution pH equal to the sample PZC. Thus, at low Mo loadings the PZC of the oxide support primarily determines the structure of hydrated surface molybdenum oxide, but at high Mo loadings the surface molybdenum oxide drastically depresses the PZC of the system.

Raman spectra of surface molybdenum oxide species under ambient conditions demonstrated that the structure of the molybdenum oxide species depends on the specific oxide

TABLE 4: Summary of XANES and Raman Structures of Surface Molybdenum Oxide Species under Ambient Conditions

		structures at low coverage		structures at high coverage	
oxide support	PZC of support	XANES	Raman	XANES	Raman
Al_2O_3	8.9	Td	MoO_4^{2-}	Oh	$Mo_7O_{24}^{6-}$,[a] $Mo_8O_{26}^{4-}$
TiO_2	6.0−6.4		$Mo_7O_{24}^{6-}$, MoO_4^{2-}	Oh	$Mo_7O_{24}^{6-}$,[a] $Mo_8O_{26}^{4-}$
ZrO_2	5.9−6.1		$Mo_7O_{24}^{6-}$, MoO_4^{2-}		$Mo_7O_{24}^{6-}$,[a] $Mo_8O_{26}^{4-}$
SiO_2	3.7−4.3	Oh	$Mo_7O_{24}^{6-}$,[a] $Mo_8O_{26}^{4-}$	Oh	$Mo_7O_{24}^{6-}$,[a] $Mo_8O_{26}^{4-}$
Nb_2O_5	4.0		$Mo_7O_{24}^{6-}$, $Mo_8O_{26}^{4-}$		$Mo_7O_{24}^{6-}$,[a] $Mo_8O_{26}^{4-}$

[a] Major species.

support and the molybdenum oxide loading. The ambient Mo L_3-edge XANES study of the molybdenum oxide coordination on the different oxide supports at low and high Mo loadings is in excellent agreement with the results derived from the ambient Raman study. The major surface molybdenum oxide species present on the oxide supports under ambient conditions at low and high Mo loading are listed in Table 4. For low Mo loading catalysts, the surface molybdenum oxide species on the Al_2O_3 support (pH at PZC = 8.9) possessed mainly monomeric species MoO_4^{2-} (Raman band at 912 cm^{-1}), and the surface molybdenum oxide species on SiO_2 (pH at PZC = 3.7−4.3) and Nb_2O_5 (pH at PZC = 4.0) were found to favor octahedral coordinated polymolybdate species such as $Mo_7O_{24}^{6-}$ and $Mo_8O_{26}^{4-}$ (Raman bands at 947 and 948 cm^{-1}, respectively; also see Table 3, $Mo_7O_{24}^{6-}$ and $Mo_8O_{26}^{4-}$ coexist at pH 2.2−4.8). The surface molybdenum oxide species on TiO_2 (pH at PZC = 6.0−6.4) and ZrO_2 (pH at PZC = 5.9−6.1) formed both tetrahedral and isolated species (MoO_4^{2-}) and polymolybdate species ($Mo_7O_{24}^{6-}$) as shown in Table 4 (Raman bands at 934 and 924 cm^{-1}, respectively). Thus, the support pH at PZC controls the molecular structures of molybdenum oxide overlayer on different oxide supports under ambient conditions at low Mo loadings.

The structural changes of the hydrated molybdenum oxide species on different oxide supports with increasing molybdenum oxide loading confirm the dependence of the surface molybdenum oxide structures on the molybdenum oxide loading which corresponds to the changes in the PZC of the samples. It was found that[23] the pH of the catalysts decreases from ~9 to ~3.7 as the Mo loading increases. The $Mo_7O_{24}^{6-}$ species coexist with the $Mo_8O_{26}^{4-}$ species at pH ~3.7 as shown in Table 3. The Raman bands of the monolayer catalysts are all located in the 947−954 cm^{-1} region, which is only slightly higher than the Raman band of the $Mo_7O_{24}^{6-}$ species (943 cm^{-1}). Therefore, the species formed on the different supports at high Mo loadings under ambient conditions are listed in Table 4, and the dominant species is $Mo_7O_{24}^{6-}$. As the molybdenum oxide content increases, the pH of their aqueous solution decreases and the ratio of $Mo_7O_{24}^{6-}/MoO_4^{2-}$ for MoO_3/Al_2O_3, MoO_3/TiO_2, and MoO_3/ZrO_2 on the support surfaces increases. The corresponding Raman shifts toward higher frequency of the terminal stretching bands of the surface molybdenum oxide species with increasing loading of the molybdenum oxides are due to these structural changes (*e.g.*, for the MoO_3/Al_2O_3 catalysts from tetrahedral to octahedral). These trends are in excellent agreement with the net surface pH at PZC model of Deo and Wachs.[79] The good agreement between the surface molybdenum oxide coordination obtained from XANES and that of the structural information from the Raman study further confirms the pH dependence. In addition, Shimada *et al.*[18] characterized the hydrated structures of molybdenum oxide on different oxide supports with EXAFS and found that a tetrahedral structure is predominant on MgO (pH at PZC = 11), an octahedral molybdenum oxide structure is present on SiO_2 and high loading TiO_2, and for Al_2O_3 the molybdenum oxide structures are tetrahedral for low loading and octahedral for high loading. Shimada *et al.*'s findings are in perfect agreement with the current Raman and XANES Mo L_3-edge studies.

The current work further suggests that the hydrated structures of surface molybdenum oxide species under ambient conditions are independent of the preparation method. In this study, the Raman spectra of the samples prepared by the aqueous impregnation method show that the net surface pH at PZC of the sample controls the structure of surface molybdenum oxide species and agrees with the studies done by Kim *et al.*[33] for supported molybdenum oxide catalysts prepared by the equilibrium adsorption method. Segawa *et al.*[57] investigated MoO_3/TiO_2 catalysts prepared by the equilibrium adsorption method by Raman and found that, at high molybdenum oxide loading and ambient conditions, octahedral coordinated molybdenum oxide species exist, which is in agreement with our results. Williams *et al.*[24,37] found that the structures of the MoO_3/Al_2O_3 and MoO_3/SiO_2 catalysts under ambient conditions were independent of the Mo precursors and the preparation pH. Machej *et al.*[64,65] found that the same hydrated molybdenum oxide structure was present for high-coverage MoO_3/TiO_2 catalysts prepared by impregnation and grafting methods. Knözinger *et al.*[7] found that the same structures are also present for molybdenum oxide dispersed on both η- and γ-Al_2O_3 supports and demonstrate that the specific structure of the oxide support also does not alter the surface structure of the ambient surface molybdenum oxide species. Thus, the molecular structures of the ambient surface metal oxide overlayers are controlled by the thermodynamics of the interactions at the hydrated metal oxide−oxide support interface. Furthermore, the ability to make the same surface molybdenum oxide overlayers from physical mixtures of crystalline MoO_3 and supports demonstrates the high mobility of the Mo species and, consequently, the lack of dependence on the preparation method.[80,82−87]

Surface Structures of Supported Molybdenum Oxides under Dehydrated Conditions. As discussed above, under ambient conditions the molecular structures of the hydrated surface molybdenum oxide species are similar to those found in aqueous solutions. At elevated temperatures, however, the adsorbed moisture desorbs from the catalyst surface and the surface becomes dehydrated. Consequently, the structures of the surface metal oxides are drastically altered upon dehydration as was found for many supported metal oxide systems (V, Nb, Cr, Re, *etc.*).[2,27,64] Unfortunately, the structures of the surface molybdenum oxide species are not the same as known solid molybdate reference compounds. As already mentioned in the Results section, unambiguous assignment of the vibrational bands for Raman spectra of solid molybdate compounds is not always straightforward since inorganic molybdenum oxide compounds possess vibrational frequencies for the tetrahedral and octahedral terminal Mo=O bond stretches that can overlap.[9,78] In addition, the stretching modes of the terminal Mo=O groups at 1046−840 cm^{-1} and of bridging Mo−O−Mo groups at 946−820 cm^{-1} can also overlap.[28,78] Moreover, the structures of many molybdate compounds cannot be classified as having

TABLE 5: Summary of XANES and Raman Structures of Surface Molybdenum Oxide under Dehydrated Conditions

oxide support	structures at low coverage		structures at high coverage	
	XANES	Raman	XANES	Raman
Al_2O_3	Td	isolated	Td + Oh	polymolybdate
TiO_2	Td + Oh[a]		Oh	polymolybdate
ZrO_2	(Td)[b]		(Td + Oh)[b]	polymolybdate
SiO_2	?	isolated	?	isolated
Nb_2O_5	(Td + Oh[a])[b]		(Oh)[b]	polymolybdate

[a] Minor species. [b] Based on similarity of Raman spectra.

precisely octahedral or tetrahedral coordination of the molybdenum ions.[78] Therefore, a Raman study of the surface molybdenum oxide species on different oxide supports under dehydrated conditions cannot provide a complete structure, but only gives some information about the Mo=O and Mo−O−Mo functionalities. However, the Mo XANES under dehydrated conditions is complementary to Raman and provides important information about the coordination of the surface molybdenum oxide species.

The Mo XANES data under dehydrated conditions indicate that there are significant differences in the local site symmetry of the surface molybdenum oxide species supported on alumina, titania, and silica brought about by dehydration. Table 5 lists the coordination of the surface molybdenum oxide species on different supports for the low loading and high loading catalysts under dehydrated conditions. For the 1% MoO_3/Al_2O_3 sample, both the splitting of the peaks and their relative intensities indicate that the surface molybdenum oxide species is tetrahedral coordinated in the dehydrated state. For the low loading MoO_3/TiO_2 sample, the spectrum also indicates that the surface molybdenum oxide species is primarily tetrahedral coordinated. However, the presence of some octahedral coordinated surface molybdenum oxide on TiO_2 cannot be excluded as the second derivative indicates the presence of a shoulder at a splitting of 3.6 eV, and the relative ratio of the intensities of the peaks is only weakly indicative of tetrahedral geometry. Thus, the dehydrated surface molybdenum oxide species present for low loading samples on Al_2O_3 and TiO_2 primarily possess tetrahedral coordination. The XANES and Raman studies of the dehydrated MoO_3/SiO_2 catalysts will be discussed separately below since the surface molybdenum oxide species on the SiO_2 support is very different from the other oxide supports.

The main Raman features upon dehydration for the supported molybdenum oxide catalysts are the disappearance of the terminal bands in the 930−960 cm^{-1} region and the appearance of very sharp bands at ~1000 cm^{-1}. The terminal Mo=O Raman stretching bands for the different supports are very similar for the dehydrated samples. At low surface coverage, the sharp Raman band at ~1000 cm^{-1} predominates, and the high-frequency position of this Raman band suggests a highly distorted structure. The absence of Raman bands in the Mo−O−Mo bending region (~220 cm^{-1}) in the spectrum of the 1% MoO_3/Al_2O_3 sample suggests that this species is isolated. The combined XANES and Raman data at low Mo loading suggest that the surface molybdenum oxide species on the Al_2O_3 support is isolated, highly distorted, and tetrahedrally coordinated. For a tetrahedrally coordinated species on the surface, the most likely structure is that possessing two terminal Mo=O bonds and two bridging Mo−O−support bonds. Accordingly, the broad ~836 cm^{-1} Raman band can be assigned to the asymmetric stretching mode of the Mo=O bonds. The Raman spectra of 1% MoO_3 on different oxide supports in the 1100−700 cm^{-1} region are compared in Figure 18a and reveal very similar features for the 1% MoO_3/ZrO_2 and 1% MoO_3/Al_2O_3 catalysts at low coverages which suggests similar structures for these two catalysts. In addition, the XANES and Raman spectra of the 1% MoO_3/TiO_2 suggest that the structures of surface molybdenum oxide are primarily highly distorted and tetrahedral coordinated species with a minor component of distorted and octahedral coordinated species. The Raman spectrum of the 1% MoO_3/Nb_2O_5 appears very similar to that of the 1% MoO_3/TiO_2, and thus, similar structures are presumably present also for these two catalysts (see Figure 18a). However, the coordinations of the dehydrated MoO_3/ZrO_2 and MoO_3/Nb_2O_5 catalysts at low loadings should be directly confirmed with further XANES measurements.

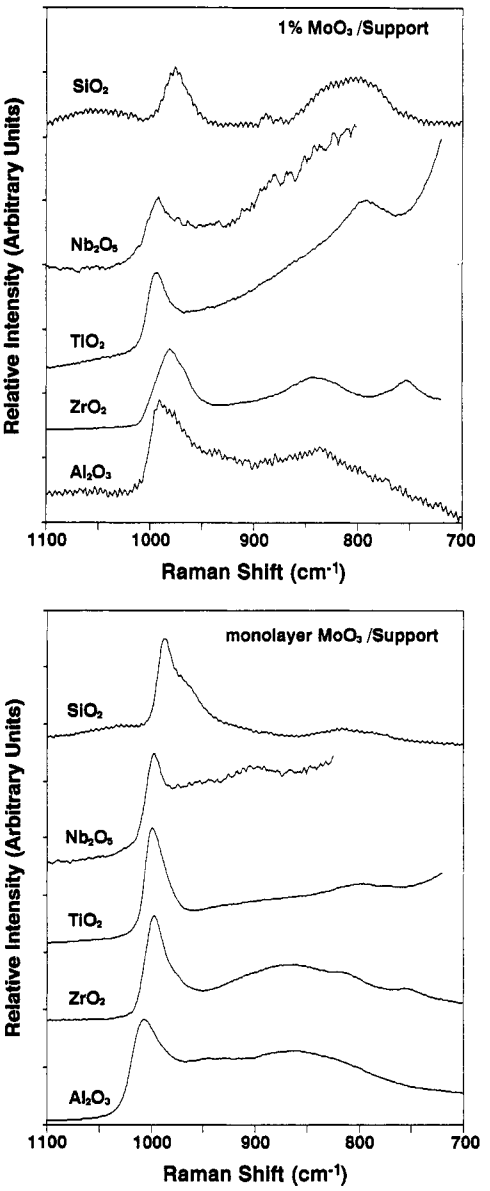

Figure 18. Raman spectra of (a, top) 1% MoO_3 catalysts on different oxide supports and (b, bottom) monolayer MoO_3 catalysts on different oxide supports under dehydrated conditions.

The XANES spectra for the monolayer coverage catalysts are quite different from their corresponding low loading catalysts. In the XANES spectrum of 18% MoO_3/Al_2O_3, the surface molybdenum oxide species appears to be octahedrally coordinated because of the large splitting of the peaks and their relative intensity ratio. However, the splitting decreases slightly compared to the spectrum of hydrated condition, and the relative ratio of the peaks becomes almost equal. While the second derivative does not clearly confirm the presence of two components in the XANES spectrum, the overall shape of the normalized spectrum is similar to that of diammonium dimolybdate in which there is an equal number of tetrahedrally and

octahedrally coordinated molybdenum oxide. On the basis of this fingerprint, at high loadings of molybdenum on alumina under dehydrated conditions there are both octahedral and tetrahedral surface molybdenum oxide species present. The XANES spectrum of the 6% MoO_3/TiO_2 sample clearly indicates the octahedral coordination of the surface molybdenum oxide species for this high loading sample. Thus, the coordination of the surface molybdenum oxide species depends on the specific oxide support.

The Raman spectra also reflect the structural changes with increasing surface molybdenum oxide coverage of the dehydrated samples. As the molybdenum oxide loading increases, a second molybdenum oxide species which possesses Raman bands at ~940, 865, 590, 377, and 210 cm^{-1} is formed on the MoO_3/Al_2O_3 catalysts at high Mo loading. The 590 and 210 cm^{-1} bands reflect the formation of Mo−O−Mo bridging bonds in the surface molybdenum oxide structure which suggests the formation of a polymerized species. For surface molybdenum oxide species on other supports, the formation of this second species is indicated by an increase of a broad Raman band at ~880 cm^{-1} that generally grows with surface molybdenum oxide coverage with the exception of SiO_2, which does not form a polymeric species (no Raman bands at ~880 and ~210 cm^{-1}). The polymeric surface molybdenum oxide species appear to be most pronounced on Al_2O_3 and ZrO_2 relative to TiO_2 and Nb_2O_5. Figure 18b compares the Raman spectra of the monolayer molybdenum oxide species on different oxide supports in the 1100−700 cm^{-1} region. The similar Raman bands for the 4% MoO_3/ZrO_2 and the 20% MoO_3/Al_2O_3 catalysts, as well as between the 5% MoO_3/Nb_2O_5 and the 6% MoO_3/TiO_2 catalysts, suggest similarities in the structures of the surface molybdenum oxide species on the respective supports. Therefore, it is concluded that, for high loadings of MoO_3/Al_2O_3 and MoO_3/ZrO_2 catalysts, highly distorted, polymerized, and octahedral coordinated surface molybdenum oxide species coexist with tetrahedral, isolated surface species. In general, the relative Raman intensity of the two dehydrated surface species, polymeric to monomeric species, increases with increasing metal oxide loading, but their relative Raman cross sections are not known. A surface highly distorted octahedral polymolybdate species is also present on the TiO_2 and Nb_2O_5 supports for high loading catalysts but does not appear to be as extensively polymerized.

From the Raman spectra of the MoO_3/SiO_2 catalysts, the surface molybdenum oxide species possesses an isolated and highly distorted structure under dehydrated conditions. De Boer *et al.*[36] found by EXAFS that total Mo−Mo coordination number decreased from 3.27 to 0.20 after dehydration, which confirms that dehydration produces essentially isolated molybdenum oxide species on SiO_2. The XANES spectra at the Mo L_3-edge of the MoO_3/SiO_2 catalysts after dehydration change quite dramatically compared to the spectra under hydrated conditions. However, there is no clear indication of splitting of the XANES white line upon dehydration, although the asymmetry of the peak clearly indicates the presence of two peaks. At present, a clear interpretation of these XANES spectra is not available. The spectra indicate that the symmetry of the molybdenum is clearly not in a slightly distorted tetrahedral or octahedral geometry as found for the other catalysts and the range of model compounds investigated. However, the similarity between the XANES spectrum of the 3.5% MoO_3/SiO_2 sample made by the nonaqueous preparation method and the 1% and 5% samples made by the aqueous impregnation method confirms the independence of the structure of the surface molybdenum oxide species on the preparation method. The symmetry of a species between tetrahedral and octahedral coordination indicated by XANES data agrees with the monooxo model suggested by the IR study that employed $^{18}O-^{16}O$ exchange to examine the MoO_3/SiO_2 catalysts.[46] According to Cornac *et al.*, the coordination of surface Mo species on SiO_2 is an octahedral species with one bridging Mo−O− bond which attaches to a surface site different from the other three Mo−O−Si bridging bonds. The remaining Mo=O bond and three Mo−O−Si bonds show tetrahedral feature. More XANES studies are needed on these samples as well as model reference compounds in order to come to a firm conclusion about the local symmetry of the dehydrated surface molybdenum oxide species on silica.

From the combined Raman and XANES data, the dehydrated structures of the surface molybdenum oxide species present on the different oxide supports at low and high loading were determined and are listed in Table 5. The results in Table 5 suggest that under dehydrated conditions the surface molybdenum oxide species tend to form isolated species on the oxide supports at low Mo loadings. When the Mo loading increases, the more dense surface Mo coverages allows polymolybdate species to be formed. For the MoO_3/SiO_2 catalysts, higher surface coverages are not possible before the formation of crystalline MoO_3, and therefore, only isolated surface molybdenum oxide species are present on this support. The isolated structures of the surface molybdenum oxide species for the low loading catalysts also suggest that the breaking of precursor clusters has occurred upon the deposition of molybdenum oxide on all oxide supports. Furthermore, this study also confirms that there is no precursor or preparation effect to the final structure of the surface molybdenum oxide species.

The combined Raman and XANES characterization techniques provide a relatively dependable determination of the structure and local site symmetry for supported molybdenum oxide catalysts. There were several recent attempts at using solid state ^{95}Mo NMR to study the structures of the surface molybdenum oxide species.[4,16,88] However, the analysis of the ^{95}Mo NMR spectrum does not appear straightforward; the variation of octahedral and tetrahedral sites affects not only the chemical shift but also the line width and line shape, and the assignment of the line shape components requires a curve-fitting program to estimate many parameters.[16,88] It appears that additional progress in solid-state ^{95}Mo NMR is required for the molecular structural assignments of supported molybdenum oxide catalysts.

Monolayer Coverage of Surface Molybdenum Oxides on Different Oxide Supports. As previously mentioned, the supported molybdenum oxide catalysts used in the present study were all prepared by the incipient-wetness impregnation method from an aqueous solution of ammonium heptamolybdate. Samples possessing only a very small Raman band at ~820 cm^{-1} are taken as representative of monolayer coverage of surface molybdenum oxide species on the specific oxide support. The Raman signal of crystalline MoO_3 is significantly stronger in comparison to the Raman signal of surface molybdenum oxide species,[28] and crystalline MoO_3 generally forms above monolayer coverage. The molybdenum oxide monolayer coverages obtained in the present study via the aqueous impregnation preparation method are listed in Table 1 for each support. Essentially the same surface density (dispersion per unit surface area) is obtained on all the oxide supports used (~4.6 Mo atoms/nm^2) with the exception of the SiO_2 support. The theoretical monolayer coverage of molybdenum oxide on an oxide support was estimated to be ~8.0 Mo atoms/nm^2, which was obtained by assuming full coverage of the support surface by a single

layer of the MoO_3 crystal phase.[60] The current findings reveal that only ~57% of a theoretical monolayer is formed for molybdenum oxide species on the oxide supports and suggests that theoretical monolayer coverage is not achievable before the formation of crystalline MoO_3. This also indicates that the theoretical model which is based on a layer of crystalline MoO_3 is not realistic since the surface molybdenum oxide species usually possess a different structure and packing density than crystalline MoO_3. A benzaldehyde–ammonia titration (BAT) method was used[89] to determine the monolayer coverages of the surface molybdenum oxide species on Al_2O_3, TiO_2, and ZrO_2 supports. A surface concentration of <7 Mo atoms/nm^2 for molybdena monolayer loading was found irrespective of the kind of support. The results are slightly higher than those from the current studies since the BAT method is less sensitive to the microcrystalline MoO_3 formation than the Raman technique.

The present work has shown that the conventional impregnation preparation gives the same dispersion as other preparation methods for oxide supports. Segawa *et al.*[57] found from the XPS Mo(3d)/Ti(2p) ratio that ~6.6 wt % MoO_3 corresponds to monolayer coverage for the TiO_2 (Degussa P-25). The close agreement between Segawa *et al.*'s results based on the equilibrium adsorption preparation method and the present result from the aqueous impregnation method (~6% MoO_3) suggests that the preparation method does not affect the final monolayer coverage. A literature search of other studies of molybdenum oxide monolayer coverage on oxide supports did not reveal higher loadings when different preparation methods were employed with the exception of the SiO_2 support (see discussion below). The current study also demonstrates that monolayer coverage is only a function of the oxide support surface area and not a function of the specific molecular structure of the surface molybdenum oxide species (*e.g.*, Oh for MoO_3/TiO_2 and Oh/Td for MoO_3/Al_2O_3).

The preparation methods and precursors do not seem to have much of an effect on the dispersion of the surface molybdenum oxide species on different oxide supports except for SiO_2 in which the nonaqueous preparation of MoO_3/SiO_2 catalysts by Williams *et al.*[37-39] did produce higher loadings of the dispersed molybdenum oxide on SiO_2. However, monolayer coverage has never been achieved on SiO_2, partially due to the low surface OH density of this support and the reactivity between adjacent silanol groups to form siloxane bridges. It has been proposed that the interaction between the precursor and the oxide support surface depends on the sign of the surface charge of the support and of the dissolved complexes of the precursor.[36] The silica surface is negatively charged at the pH of the AHM solution (~5.5) and is thought to account for the lack of interaction with the anionic heptamolybdate cluster. However, in the present study the same monolayer coverage of surface molybdenum oxide species on the Nb_2O_5 support (PZC ~ 4) as on the other oxide supports was also obtained, which suggests that the surface charge of the support is not the controlling factor for the dispersion of molybdenum oxide. The spontaneous dispersion behavior[82-87] of molybdenum oxide on the surface of oxide supports with the exception of SiO_2 suggests it is more likely that there is a driving force for the dispersion of molybdenum oxide on the surface of oxide supports. The inability to form monolayer coverage of surface molybdenum oxide species on SiO_2, however, reflects a repulsion between the SiO_2 surface and metal oxides since physical mixtures of surface molybdenum oxide species on SiO_2 and other oxide supports (TiO_2, Al_2O_3, *etc.*) result in complete migration of the surface molybdenum oxide species away from the SiO_2 support upon heating (*e.g.*, $MoO_3/SiO_2 + TiO_2 \rightarrow SiO_2 + MoO_3/TiO_2$).[90]

Conclusions

The molecular structures of the surface molybdenum oxide species on the Al_2O_3, TiO_2, ZrO_2, Nb_2O_5, and SiO_2 supports were investigated by Raman and XANES at the Mo L_3-edge spectroscopies as a function of Mo loading and hydration/dehydration states.

Under ambient conditions, the structures of supported molybdenum oxide species resembles molybdate species in aqueous solutions. At low Mo loadings, the structure of surface molybdenum oxide species depends on the pH at the point of zero charge of the different supports. At high Mo loadings, the structure of surface molybdenum oxide species also depends on the molybdenum oxide coverage, which decreases the pH at the point of zero charge of the catalyst surface. For molybdenum oxide supported on SiO_2 and Nb_2O_5 supports, hydrated polymolybdate clusters ($Mo_7O_{24}^{6-}$ and $Mo_8O_{26}^{4-}$) are the principal species present on the surfaces. For the TiO_2 and ZrO_2 supported molybdenum oxide, the major species are tetrahedral species (MoO_4^{2-}) at low Mo loadings and polymolybdates ($Mo_7O_{24}^{6-}$) at high Mo loadings. For the Al_2O_3 support, at low loadings the isolated and tetrahedral coordinated molybdenum oxides (MoO_4^{2-}) are the main species, and the polymeric species ($Mo_7O_{24}^{6-}$) increase with Mo loadings. The molecular structures of the hydrated surface molybdenum oxide species can be predicted by the pH at PZC model.

Under dehydrated conditions, the structures of the surface molybdenum oxide species depend on both the specific oxide support and the Mo loading. A highly distorted and isolated structure are observed to be present on all supports at low loading. On the Al_2O_3 support, this species is tetrahedrally coordinated; on the TiO_2 support the major species are also tetrahedral coordinated. At high loadings, octahedral coordinated polymolybdate species as well as isolated tetrahedral species are present on the surface of Al_2O_3, but the polymolybdate species predominate on the TiO_2 support. The structures of the MoO_3/ZrO_2 appear to be similar to that of the MoO_3/Al_2O_3, and the structures of the MoO_3/Nb_2O_5 appear to be similar to that of the MoO_3/TiO_2. The SiO_2 supported surface molybdenum oxide species are isolated and highly distorted at all loadings and possess a symmetry somewhat between octahedral and tetrahedral coordinations, and additional studies with molybdenum oxide reference compounds are required.

Acknowledgment. The authors gratefully acknowledge the helpful discussion with members of our research group and thank Dr. N. D. Spencer for the ICP Mo analysis of the catalysts. Financial support by The National Science Foundation, Grant CTS-9006258, is also gratefully acknowledged. The XANES measurements were performed at the NSLS, Brookhaven National Laboratory, which is supported by DOE under contract DC-AC02-76CH00016.

References and Notes

(1) Haber, J. *The Role of Molybdenum in Catalysis*; Climax Molybdenum Co.: Ann Arbor, MI, 1981.

(2) Segawa, K.; Wachs, I. E. In *Characterization of Catalytic Materials*; Wachs, I. E., Ed.; Butterworth-Heinemann: Boston, 1992; p 72.

(3) Bartlett, J. R.; Cooney, R. P. In *Spectroscopy of Inorganic-Based Materials*; Clark, R. J. H., Hester, R. E., Eds.; John Wiley & Sons: New York, 1987; p 187.

(4) Han, O. H.; Lin, C. Y.; Sustache, N.; McMillan, M.; Carruthers, J.

D.; Zilm, K. W.; Haller, G. L. *Appl. Catal. A: Gen.* **1993**, *98*, 195.
(5) Stencel, J. M. In *Raman Spectroscopy for Catalysis*; Van Nostrand Reinhold: New York, 1990; p 51.
(6) Medema, J.; van Stam, C.; de Beer, V. H. J.; Konings, A. J. A.; Koningsberger, D. C. *J. Catal.* **1978**, *53*, 386.
(7) Knözinger, H.; Jeziorowski, H. *J. Phys. Chem.* **1978**, *82*, 2002.
(8) Jeziorowski, H.; Knözinger, H. *J. Phys. Chem.* **1979**, *83*, 1166.
(9) Wang, L.; Keith Hall, W. *J. Catal.* **1980**, *66*, 251.
(10) Wang, L.; Keith Hall, W. *J. Catal.* **1983**, *83*, 242.
(11) Jeziorowski, H.; Knözinger, H.; Grange, P.; Gajardo, P. *J. Phys. Chem.* **1980**, *84*, 1825.
(12) Cornac, M.; Janin, A.; Lavalley, J. C. *Infrared Phys.* **1984**, *24*, 143.
(13) Okamoto, Y.; Imanaka, T. *J. Phys. Chem.* **1988**, *92*, 7102.
(14) Rodrigo, L.; Marcinkowska, K.; Adnot, A.; Roberge, P. C.; Kaliaguine, S.; Stencel, J. M.; Makovsky, L. E.; Diehl, J. R. *J. Phys. Chem.* **1986**, *90*, 2690.
(15) Zingg, D. S.; Makovsky, L. E.; Tischer, R. E.; Brown, F. R.; Hercules, D. M. *J. Phys. Chem.* **1980**, *84*, 2898.
(16) Edwards, J. C.; Adams, R. D.; Ellis, P. D. *J. Am. Chem. Soc.* **1990**, *112*, 8349.
(17) Luthra, N. P.; Cheng, W.-C. *J. Catal.* **1987**, *107*, 154.
(18) Shimada, H.; Matsubayashi, N.; Sato, T.; Yoshimura, Y.; Nishijama, A.; Kosugi, N.; Kuroda, H. *J. Catal.* **1992**, *138*, 746.
(19) Cheng, C. P.; Schrader, G. L. *J. Catal.* **1979**, *60*, 276.
(20) Ng, K. Y. S.; Zhou, X.; Gulari, E. *J. Phys. Chem.* **1985**, *89*, 2477.
(21) Hall, W. K. *J. Proc. Climax 4th Int. Conf. Chem. Uses Molybdenum* **1982**, 224.
(22) Payen, E.; Grimblot, J.; Kasztelan, S. *J. Phys. Chem.* **1987**, *91*, 6642.
(23) Kohler, S. D.; Ekerdt, J. G.; Kim, D. S.; Wachs, I. E. *Catal. Lett.* **1992**, *16*, 231.
(24) Williams, C. C.; Ekerdt, J. G.; Jehng, J.-M.; Hardcastle, F. D.; Wachs, I. E. *J. Phys. Chem.* **1991**, *95*, 8791.
(25) Stencel, J. M.; Makovsky, L. E.; Sarkus, T. A.; de Vries, J.; Thomas, R.; Moulijn, J. A. *J. Catal.* **1984**, *90*, 314.
(26) Payen, E.; Kasztelan, S.; Grimblot, J.; Bonnelle, J. P. *J. Raman Spectrosc.* **1986**, *17*, 233.
(27) Chan, S. S.; Wachs, I. E.; Murrell, L. L.; Wang, L.; Keith Hall, W. *J. Phys. Chem.* **1984**, *88*, 5831.
(28) Vuurman, M. A.; Wachs, I. E. *J. Phys. Chem.* **1992**, *96*, 5008.
(29) Vuurman, M. A.; Wachs, I. E. *J. Mol. Catal.* **1992**, *77*, 29.
(30) Gao, X.; Xin, Q. *Catal. Lett.* **1993**, *18*, 409.
(31) Diaz, A. L.; Bussell, M. E. *J. Phys. Chem.* **1993**, *97*, 470.
(32) Smith, M. R.; Zhang, L.; Driscoll, S. A.; Ozkan, U. S. *Catal. Lett.* **1993**, *19*, 1.
(33) Kim, D. S.; Segawa, K.; Soeya, T.; Wachs, I. E. *J. Catal.* **1992**, *136*, 539.
(34) Martín, C.; Martín, M.; Rives, V. *Stud. Surf. Sci. Catal.* **1992**, *72*, 415.
(35) Liu, T. C.; Forissier, M.; Coudurier, G.; Védrine, J. C. *J. Chem. Soc., Faraday Trans. 1* **1989**, *85*, 1607.
(36) de Boer, M.; van Dillen, A. J.; Koningsberger, D. C.; Geus, J. W.; Vuurman, M. A.; Wachs, I. E. *Catal. Lett.* **1991**, *11*, 227.
(37) Williams, C. C.; Ekerdt, J. G.; Jehng, J.-M.; Hardcastle, F. D.; Turek, A. M.; Wachs, I. E. *J. Phys. Chem.* **1991**, *95*, 8781.
(38) Roark, R. D.; Kohler, S. D.; Ekerdt, J. G.; Kim, D. S.; Wachs, I. E. *Catal. Lett.* **1992**, *16*, 77.
(39) Roark, R. D.; Kohler, S. D.; Ekerdt, J. G. *Catal. Lett.* **1992**, *16*, 71.
(40) Barbaux, Y.; Elamrani, A. R.; Payen, E.; Gengembre, L.; Bonnelle, J. P.; Grzybowska, B. *Appl. Catal.* **1988**, *44*, 117.
(41) Kasztelan, S.; Payen, E.; Moffat, J. B. *J. Catal.* **1988**, *112*, 320.
(42) Rocchiccioli-Deltcheff, C.; Amirouche, M.; Che, M.; Tatibouët, J. M.; Fournier, M. *J. Catal.* **1990**, *125*, 292.
(43) Stencel, J. M.; Diehl, J. R.; D'Este, J. R.; Makovsky, L. E.; Rodrigo, L.; Marcinkowska, K.; Adnot, A.; Roberge, P. C.; Kaliaguine, S. *J. Phys. Chem.* **1986**, *90*, 4739.
(44) Seyedmonir, S. R.; Howe, R. F. *J. Catal.* **1988**, *110*, 216.
(45) Wachs, I. E.; Deo, G.; Kim, D. S.; Vuurman, M. A.; Hu, H. *Proc. Int. Congr. Catal. 10th, A* **1992**, 543.
(46) Cornac, M.; Janin, A.; Lavalley, J. C. *Polyhedron* **1986**, *5*, 183.
(47) Seyedmonir, S. R.; Abdo, S.; Howe, R. F. *J. Phys. Chem.* **1982**, *86*, 1233.
(48) Marcinowska, K.; Rodrigo, L.; Kaliaguine, S.; Roberge, P. C. *J. Catal.* **1986**, *97*, 75.
(49) Hazankamp, M. F. Ph.D. Thesis, University of Utrecht, The Netherlands, 1992.
(50) Louis, C.; Che, M.; Anpo, M. *J. Catal.* **1993**, *141*, 453.
(51) Bañares, M. A.; Fierro, J. L. G. *Catal. Lett.* **1993**, *17*, 205.
(52) Aigler, J. M.; Brito, J. L.; Leach, P. A.; Houalla, M.; Proctor, A.; Cooper, N. J.; Hall, W. K.; Hercules, D. M. *J. Phys. Chem.* **1993**, *97*, 5699.
(53) Louis, C.; Che, M. *J. Catal.* **1992**, *135*, 156.
(54) Ono, T.; Anpo, M.; Kubokawa, Y. *J. Phys. Chem.* **1986**, *90*, 4780.
(55) Datta, A. K.; Ha, J. W.; Regalbuto, J. R. *J. Catal.* **1992**, *133*, 55.
(56) Spanos, N.; Matralis, H. K.; Kordulis, C.; Lycourghiotis, A. *J. Catal.* **1992**, *136*, 432.
(57) Segawa, K.; Soeya, T.; Kim, D. S. *Sekiyu Gakkaishi* **1990**, *33*, 347.
(58) Ng, K. Y. S.; Gulari, E. *J. Catal.* **1985**, *92*, 340.
(59) Ono, T.; Nakagawa, Y.; Miyata, H.; Kubokawa, Y. *Bull. Chem. Soc. Jpn.* **1984**, *57*, 1205.
(60) Bond, G. C.; Flamerz, S.; Wijk, L. V. *Catal. Today* **1987**, *1*, 229.
(61) Quincy, R. B.; Houalla, M.; Hercules, D. M. *J. Catal.* **1987**, *106*, 85.
(62) Quincy, R. B.; Houalla, M.; Proctor, A.; Hercules, D. M. *J. Phys. Chem.* **1989**, *93*, 5882.
(63) van Hengstum, A. J.; van Ommen, J. G.; Bosch, H.; Gellings, P. J. *Appl. Catal.* **1983**, *5*, 207.
(64) Machej, T.; Doumain, B.; Yasse, B.; Delmon, B. *J. Chem. Soc., Faraday Trans. 1* **1988**, *84*, 3905.
(65) Machej, T.; Haber, J.; Turek, A. M.; Wachs, I. E. *Appl. Catal.* **1991**, *70*, 115.
(66) Ono, T.; Miyata, H.; Kubokawa, Y. *J. Chem. Soc., Faraday Trans. 1* **1987**, *83*, 1761.
(67) Miyata, H.; Tokuda, S.; Ono, T.; Ohno, T.; Hatayama, F. *J. Chem. Soc., Faraday Trans. 1* **1990**, *86*, 2291.
(68) Jin, Y. S.; Ouqour, A.; Auroux, A.; Védrine, J. C. In *Structure and Reactivity of Surfaces*; Morterra, C., Zecchina, A., Costa, G., Eds.; Elsevier: Amsterdam, 1989; p 525.
(69) Jehng, J.-M.; Turek, A. M.; Wachs, I. E. *Appl. Catal. A: Gen.* **1992**, *83*, 179.
(70) López Cordero, R.; Gil-Lliambias, F. J.; López Agudo, A. *Appl. Catal.* **1991**, *74*, 125.
(71) Cáceres, C. V.; Fierro, J. L. G.; Lázaro, J.; López Agudo, A.; Soria, J. *J. Catal.* **1990**, *122*, 113.
(72) Bare, S. R.; Mitchell, G. E.; Maj, J. J.; Vrieland, G. E.; Gland, J. L. *J. Phys. Chem.* **1993**, *97*, 6048.
(73) Hedman, B.; Penner-Hahn, J. E.; Hodgson, K. O. In *EXAFS and Near Edge Structure III*; Hodgson, K. O., Hedman, B., Penner-Hahn, J. E., Eds.; Springer-Verlag: Berlin, 1984.
(74) George, G. N.; Cleland, W. E.; Enemark, J. H.; Smith, B. E.; Kipke, C. A.; Roberts, S. A.; Cramer, S. P. *J. Am. Chem. Soc.* **1988**, *110*, 3798.
(75) The EXAFS Company, Seattle, WA.
(76) Lytle, F. W.; Greegor, R. B.; Marques, E. C. *Proc. 9th Int. Congr. Catal.* **1988**, *5*, 54.
(77) Jeziorowski, H.; Knözinger, H. *J. Phys. Chem.* **1979**, *83*, 1166.
(78) Hardcastle, F. D.; Wachs, I. E. *J. Raman Spectrosc.* **1990**, *21*, 683.
(79) Deo, G.; Wachs, I. E. *J. Phys. Chem.* **1991**, *95*, 5889.
(80) Leyrer, J.; Mey, D.; Knözinger, H. *J. Catal.* **1990**, *124*, 349.
(81) Butler, M. A.; Ginley, D. S. *J. Electrochem. Soc.* **1978**, *125*, 228.
(82) Stampfl, S. R.; Chen, Y.; Dumesic, J. A.; Niu, C.; Hill, C. G., Jr. *J. Catal.* **1987**, *105*, 445.
(83) Knözinger, H.; Taglaner, E. *Catal. Pre. R. Soc. Chem.* **1993**, *10*, 1.
(84) Leyrer, J.; Zaki, M. I.; Knözinger, H. *J. Phys. Chem.* **1986**, *90*, 4775.
(85) Reddy, B. M.; Reddy, E. P.; Srinivas, S. T. *J. Catal.* **1992**, *136*, 50.
(86) Kisfaludi, G.; Leyrer, J.; Knözinger, H.; Prins, R. *J. Catal.* **1991**, *130*, 192.
(87) del Arco, M.; Carrazán, S. R. G.; Rives, V.; Gill-Llambías, F. J.; Malet, P. *J. Catal.* **1993**, *141*, 48.
(88) Edwards, J. C.; Zubieta, J.; Shaikh, S. N.; Chen, Q.; Bank, S.; Ellis, P. D. *Inorg. Chem.* **1990**, *29*, 3381.
(89) Matsuoka, Y.; Niwa, M.; Murakami, Y. *J. Phys. Chem.* **1990**, *94*, 1477.
(90) Jehng, J.-M.; Wachs, I. E. Unpublished results.

JP950016P